Received: 30 April 2022 | Revised: 4 June 2022 | Accepted: 19 June 2022

DOI: 10.1002/idm2.12049

REVIEW

Interdisciplinary Materials — Open Access — WILEY

Metamaterials: From fundamental physics to intelligent design

Ji Chen[1,2] | **Shanshan Hu**[1] | **Shining Zhu**[1] | **Tao Li**[1]

[1]National Laboratory of Solid State Microstructures, Key Laboratory of Intelligent Optical Sensing and Manipulations, Jiangsu Key Laboratory of Artificial Functional Materials, College of Engineering and Applied Sciences, School of Physics, Nanjing University, Nanjing, China

[2]National Mobile Communications Research Laboratory, School of Information Science and Engineering, Frontiers Science Center for Mobile Information Communication and Security, Southeast University, Nanjing, China

Correspondence
Tao Li, Ji Chen, and Shining Zhu, National Laboratory of Solid State Microstructures, Key Laboratory of Intelligent Optical Sensing and Manipulations, Jiangsu Key Laboratory of Artificial Functional Materials, College of Engineering and Applied Sciences, School of Physics, Nanjing University, 210093 Nanjing, China.
Email: taoli@nju.edu.cn, jichen@seu.edu.cn, and zhusn@nju.edu.cn

Funding information
National Key R&D Program of China, Grant/Award Number: 2016YFA0202103; Fundamental Research Funds for the Central Universities, Grant/Award Numbers: 2242022R10128, 2242022k30006; National Natural Science Foundation of China, Grant/Award Numbers: 12104223, 91850204

Abstract

Metamaterials are artificial structures with the ability to efficiently control light-field, attracting intensive attention in the past few decades. People have studied the working principles, design strategies, and fabrication methods of metamaterials, making this field cross and combine with many disciplines, including physics, material science, electronics, and chemistry. In recent years, with the rapid development of high-efficiency and multifunctional metasurfaces, which are a two-dimensional version of metamaterials, great efforts have been made to push this material to practical applications. In particular, the introduction of artificial intelligent (AI) algorithms enables metamaterials-based photonic devices that exhibit excellent performances and intelligent functionalities. In this review, we first introduce the basic concepts, working principles, design methods, and applications of metamaterials, and then focus on the rapidly developing metamaterials research combined with AI algorithms. Finally, we conclude this review with personal perspectives on the current problems and future directions of metamaterials research and developments.

KEYWORDS
artificial intelligence, artificial neural network, inverse design, metamaterial, metasurface

1 | INTRODUCTION

The ability to efficiently manipulate electromagnetic (EM) waves is always highly desired for its great significance in many aspects, like, imaging, information communications, target detection, energy utilizations, and optical encryptions. Conventional optical components are composed of natural materials, such as lenses, waveplates, and polarizers, and possess a very limited range of permittivity, leading to their bulky size, and curved shapes to ensure enough accumulation of propagating phase. However, it is still far from satisfying people's desire for arbitrary manipulation of EM waves. Metamaterials are artificial materials composed of an array of nanostructures, which function as the atoms and molecules in traditional materials and are termed as meta-atoms. Different from

natural materials, the properties of metamaterials are not determined by the intrinsic properties of chemical constituents but rather determined by the specific structures of meta-atoms.[1,2] Through efficient interactions between incident EM waves and the meta-atoms, metamaterials possess powerful light-field manipulation ability and exhibit fascinating physical properties some of which are even not achievable in natural existing materials.[3–8]

If we describe all materials in parameter space with axes of permittivity (ε) and permeability (μ) (Figure 1A), which are two basic parameters to describe how EM fields interact with materials,[9] most dielectric materials will locate in the quadrant where ε and μ are all positive. Quadrant with $\varepsilon < 0$ and $\mu > 0$ covers materials of metals and ferroelectric materials, while some ferrite materials are included in the opposite quadrant with $\varepsilon > 0$ and $\mu < 0$. However, natural existing materials with simultaneously negative permittivity and permeability have not been found so far. Through careful structural design, in principle metamaterials can exhibit arbitrary values of ε and μ, which leads to the significant capability of metamaterials to control EM waves. Therefore despite Veselago theoretically investigated materials with simultaneously negative permittivity and permeability as early as 1968,[10] this kind of material was eventually achieved by using metamaterials after several decades. However, despite metamaterials possessing the strong ability to manipulate light fields, the nonnegligible losses and the fabrication challenges of complicated three-dimensional (3D) structures hinder its development toward practical applications.

Metasurfaces are generally created by using optically thin films and assembled by arrays of subwavelength scatterers, which can be viewed as a two-dimensional (2D) version of metamaterials. The working principles of metasurfaces are totally different from 3D metamaterials in that metasurfaces break out the dependence of propagating effect inside the metamaterials by introducing abrupt changes of optical properties which are achieved by interactions between light and scatterers.[11–14] Through arranging scatterers with various geometric parameters in certain arrays, spatially varying optical responses can be formed at will. Owing to the advantages like ultrathin thickness, relatively low fabrication difficulty, and low-loss optical field modulation, metasurfaces have been extensively studied in recent years and shown promising prospects in realistic applications.[15–28] Numerous functionalities have been demonstrated, such as metalens, beam engineering, waveplates, polarizers, and holograms, the performances of which strongly rely on the design, and optimization of metastructures.

With the continuous development of metamaterials and metasurfaces, researchers have gradually shifted their attention from explorations of new physical principles to versatile functionalities and devices based on this newly emerging optical design. Thus various optimization algorithms are used to seek the optimal structure parameters for realizing specific functions.[29–31] However, due to the more and more complex desired functions and growing demands on the devices' performances, simple and regular meta-atoms will no longer meet the requirements, instead of sophisticated structures being used to construct the metadevices. This will undoubtedly lead to a very large space of parameters that can hardly be optimized by traditional algorithms. In recent years, artificial intelligence (AI) algorithms especially artificial neural networks (ANNs) have been successfully applied in complex metastructures designing, endowing the metadevices with richer functions, and excellent performances.[32–34] This successful combination points to a promising direction of metadevices development, hence in this review, we will pay much attention and fully discussion to this direction.

This review is organized as follows, after introducing the basic concepts and development trend of metamaterials

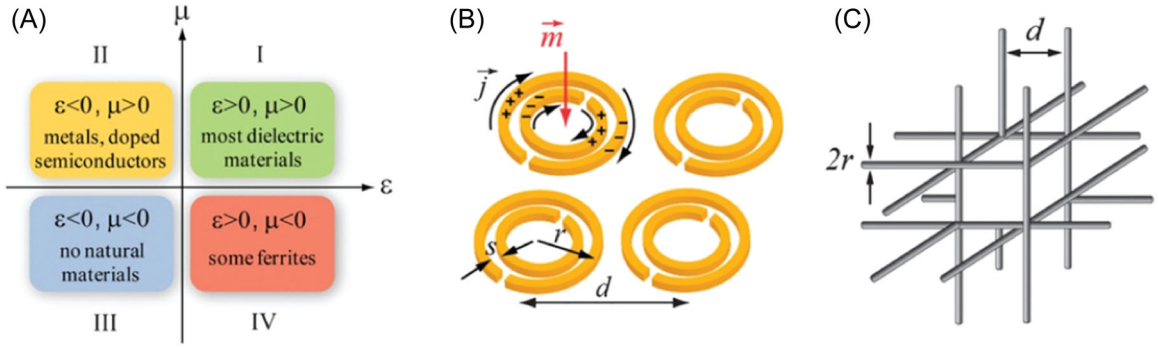

FIGURE 1 Working principles of three-dimensional (3D) metamaterials. (A) Material parameter space characterized by permittivity and permeability. (B) Schematic of split-ring resonators. (C) Schematic of periodic infinite wires. Three figures are all reproduced with permission.[7] Copyright 2011, Royal Society of Chemistry.

in Section 1, successively we present the working principles and applications of 3D metamaterials and metasurfaces in Sections 2 and 3, respectively. Subsequently, traditional structural design methods including numerical simulations and classical optimization algorithms are introduced in Section 4. Following in Section 5 is the focus of this review, AI design methods which will be discussed in detail to show how metamaterials are endowed with the properties of intelligence. Finally, in Section 6 this review is concluded with personal perspectives on the current problems and future directions of this rapidly growing research field.

2 | WORKING PRINCIPLES OF 3D METAMATERIALS AND THEIR APPLICATIONS

2.1 | Working principles

Permittivity (ε) and permeability (μ) are two basic parameters of materials to describe the EM responses to external EM waves, which usually can be described by the Drude–Lorentz model shown as[9]

$$\begin{cases} \varepsilon_r(\omega) = 1 - \dfrac{\omega_{p,e}^2}{\omega^2 - \omega_{0,e}^2 + i\gamma_e\omega}, \\ \mu_r(\omega) = 1 - \dfrac{\omega_{p,m}^2}{\omega^2 - \omega_{0,m}^2 + i\gamma_m\omega}, \end{cases} \tag{1}$$

Here ω_p, ω_0, and γ are the plasma frequency, the resonant frequency, and the damping factor with subscripts 'e' and 'm' represent electric and magnetic response, respectively. In naturally existing materials these parameters are generally fixed which are related to the intrinsic properties of the materials. Taking noble metals as an example, $\omega_{0,e}$ is taken as zero under the free electron approximation, which means the permittivity of metals is always negative below the plasma frequency. On the contrary, the permittivity of dielectric materials is almost positive. In contrast to the apparent electrical responses to incident light, the magnetic response in natural substances is significantly weaker at optical frequency, leading to the magnetic permeability being nearly unity, that is, $\mu = 1$ holds for all naturally existing materials.

Metamaterials are artificial structures that allow us to tailor the EM material properties to a previously unprecedented degree. That is permittivity and permeability can be controlled using properly designed structures. Thanks to this complete freedom, it is possible to design metamaterials to surmount obstacles of nature, such as magnetism at optical frequencies. By mimicking a usual liquid crystal (LC) circuit, consisting of a plate capacitor with capacitance C and a magnetic coil with inductance L, people have successfully realized artificial magnetic "atoms," termed split-ring resonators (SRRs; Figure 1B). A magnetic field penetrating the resonator will induce a strong circulating current and thus result in an effective magnetic moment.[35–38] The effective capacitance C and inductance L of SRRs are related to the structure parameters marked in the figure, which are shown as $C = \varepsilon_0\varepsilon_C\omega t/d$ and $L = \mu_0 l^2/t$, respectively. These lead to the eigenfrequency

$$\omega_0 = \frac{1}{\sqrt{LC}} = \frac{1}{l}\frac{\varepsilon_0}{\sqrt{\varepsilon_C}}\sqrt{\frac{d}{\omega}}. \tag{2}$$

John Pendry derived the effective relative magnetic permeability of an SRR array which is given by[39]

$$\mu_{r,\mathrm{eff}}(\omega) = 1 - \frac{F\omega^2}{\omega^2 - \omega_0^2 + i\Gamma\omega}, \tag{3}$$

where F is the filling ratio of the SRR and Γ is the damping term. If the magnetic response of the SRR is sufficiently strong, $\mu_{r,\mathrm{eff}}$ with a negative value can be achieved.

In addition to SRR, Pendry et al. also proposed basic metamaterial structures to implement artificial electric responses that are dilute metals with extremely low plasma frequency.[40] The structure is composed of periodic infinite wires arranged in a simple cubic lattice (Figure 1C). Detailed derivations show that the effective permittivity of the system is given by

$$\varepsilon_{r,\mathrm{eff}} = 1 - \frac{\omega_{p,\mathrm{eff}}^2}{\omega(\omega + i\gamma_{\mathrm{eff}})}, \tag{4}$$

where $\omega_{p,\mathrm{eff}}^2$, and γ_{eff} are, respectively, the effective plasma frequency and damping factor which are related with the structure parameters, shown as $\omega_{p,\mathrm{eff}}^2 = \frac{2\pi c^2}{d^2\ln(d/r)}$ and $\gamma_{\mathrm{eff}} = \frac{\varepsilon_0 d^2\omega_p^2}{\pi r^2\sigma}$, respectively.

2.2 | Negative-index metamaterials

By using the combination of periodic SRR and wires as the basic structure, the composed metamaterials will exhibit any desired permittivity and permeability after well determining the structural parameters. A representative example is the realization of negative-index metamaterials with $\varepsilon < 0$ and $\mu < 0$, which was proposed by Veselago

many decades ago.[10] Figure 2A shows the schematic of negative refraction phenomena. Smith's group first experimentally demonstrated negative-index metamaterials at the microwave frequency, by designing the structure consisting of a periodic array of copper SRRs and wires (Figure 2B). Negative refraction was observed in a manner consistent with Snell's law in their work.[41,48] Since then, magnetic metamaterials and negative-index metamaterials have aroused strong research interest, a series of related works were reported within several years. The working wavelengths of the realized metamaterials covered not only the microwave but also the visible

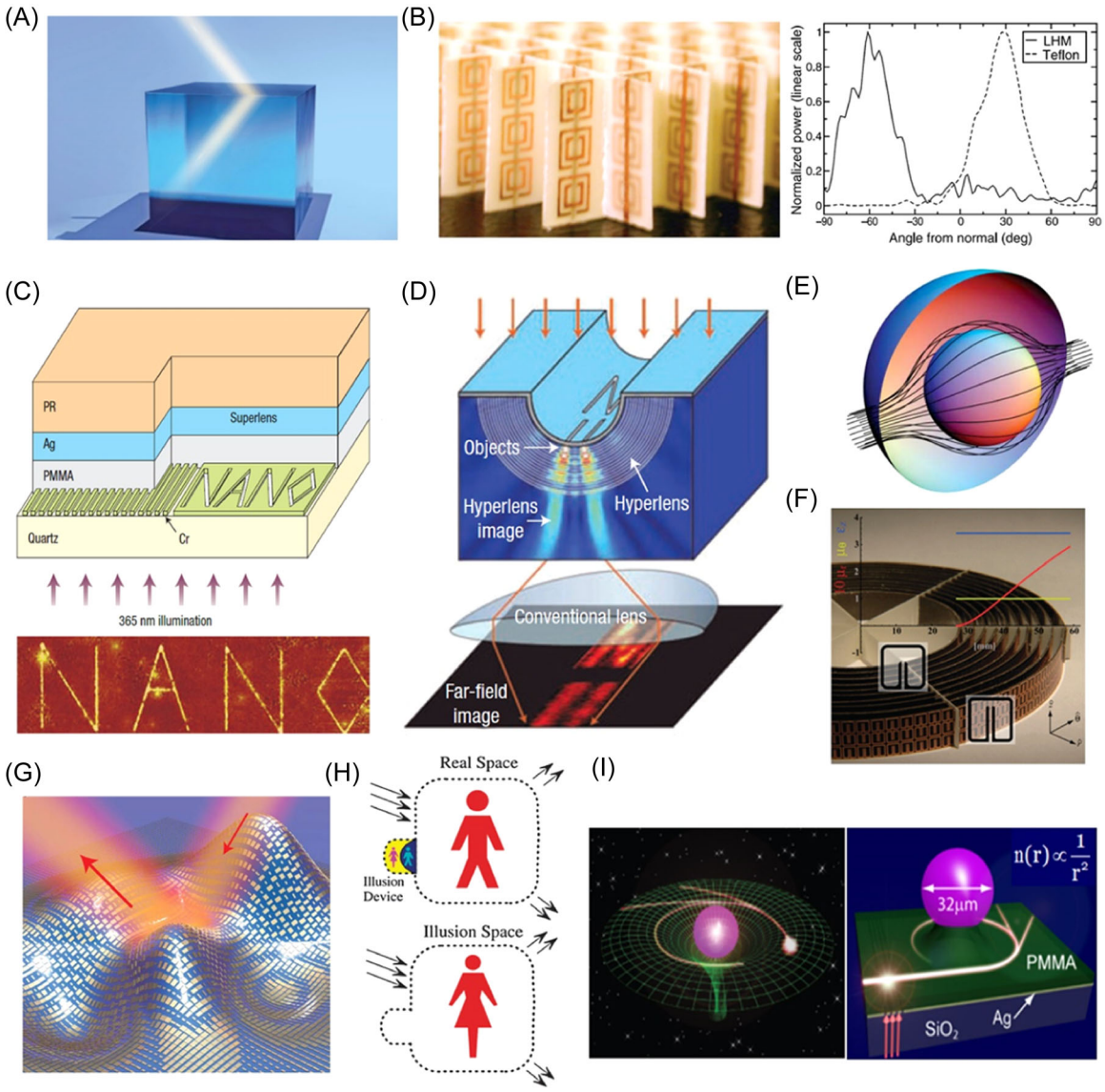

FIGURE 2 Applications of metamaterials. (A) Schematic of negative refraction phenomenon. (B) Negative-index metamaterials (left) and the experimental results (right) working at microwave frequencies. Reproduced with permission.[41] Copyright 2001, American Association for the Advancement of Science. (C) Optical superlensing experiment. Reproduced with permission.[42] Copyright 2005, American Association for the Advancement of Science. (D) Schematic of the experimental setup for hyperlens demonstration. Reproduced with permission.[43] Copyright 2007, American Association for the Advancement of Science. (E) Light propagating through the cloaking material. Reproduced with permission.[44] Copyright 2006, American Association for the Advancement of Science. (F) Experimental setup for cloaking at microwave frequency. Reproduced with permission.[45] Copyright 2006, American Association for the Advancement of Science. (G) Illustration of a metasurface skin cloak. Reproduced with permission.[21] Copyright 2015, American Association for the Advancement of Science. (H) The working principle of an illusion device that transforms the stereoscopic image of the object (a man) into that of the illusion (a woman). Reproduced with permission.[46] Copyright 2009, American Physical Society. (I) Analogue of light deflection in a gravitational field (left) and microstructured optical waveguide (right). Reproduced with permission.[47] Copyright 2013, Springer Nature.

regime.[37,49–51] However, due to the very shot working wavelength at visible, the structure size of SRR is also drastically reduced, which not only brings great challenges to fabrication but also ultimately affects the magnetic response in SRR.

To circumvent this difficulty, researchers used fishnet structure[52,53] as an alternative design to realize negative-index materials other than a combination of metal wires and SRRs, which are composed of two layers of metal meshes with a dielectric spacer layer in the middle, as shown in the figure. The top and bottom metal films form a loop and the induced current is interrupted by the hole which also forms a capacitor between the two films giving a resonant permeability response. Thus the paired stripes oriented parallel to the electric field provide negative permittivity while the pairs of stripes parallel to the magnetic field offer negative permeability. This fishnet structure is much easier to fabricate than the combination of metal wires and SRRs, providing a new direction for the design of negative refractive index materials.

One of the most striking properties of negative-index material is that a slab negative-index material can be a "perfect lens" in which the evanescent waves, instead of decaying, are in fact enhance through the slab.[54] This offers the possibility to make a perfect image without any deterioration, which was first proposed by Pendry.[55] The evanescent waves of a light passing through an object always carry the subwavelength detail of the object. However, the evanescent waves decay exponentially in mediums with a positive refractive index so that they cannot be collected at the image plane by a conventional lens, resulting in a diffraction-limited image. But the evanescent waves propagating in a negative-index material will have opposite behavior that is the evanescent waves can be strongly enhanced across the media. So if the middle of the object plane and the image plane is filled with a proper combination of positive- and negative-index slabs, the object wave can be completely recovered to form a perfect image on the image plane, as shown in the figure. After Pendry proposed the concept, researchers used various kinds of metamaterials structure to realize superlens and experimentally demonstrated the perfect imaging at microwave and optical frequencies (Figure 2C,D).[42,43,56]

2.3 | Transformation optics

In addition to negative refractive index materials, another important research field of metamaterials is transformation optics, the goal of which is to precisely control the flow of light in desirable manners by spatially tailoring the material property.[57–59] The invariance of Maxwell's equations implies that the coordinate transformation can instead be applied to the permittivity and permeability, giving rise to the prescription of the spatial profile of the material that enables us to achieve desired light flow. Following rigorous mathematical derivation to design metamaterials for transformation optics, researchers have been able to realize many exotic optical phenomena, including invisible cloak, illusion optics, and optical black holes.

Transformation optics render an object invisible by guiding the flow of light around the hidden object without disturbance to the internal object (Figure 2E). In 2006, transformation optics for cloaking was independently presented by Pendry et al.[44] and Leonhardt.[60] Soon after a 2D cloak prototype composed of SRRs was designed in an experiment to validate cloaking phenomena in the microwave spectrum (Figure 2F).[45] Besides the complete cloak, the carpet cloak aiming to give all cloaked objects the appearance of a flat conducting sheet was extensively studied since first proposed by Li and Pendry.[61] Carpet cloak relieves the loss issue by avoiding the usage of resonating elements hence is easier to be realized at optical frequencies (Figure 2G).[62–65] More than in EM waves, transformation optics have been used as a universal tool to engineer sound, heat flow, elastic waves, water waves, and so on.[66–71] Illusion optics could transform an object into an illusion of another object (Figure 2H) by using the complementary medium and the restoring medium designed from transformation optics.[46,58] To achieve a total illusion effect for all angles, the far-field EM responses of the original object plus the illusion device must be equal to the illusion object for any incident waves. However, it is far from being implemented experimentally, as it requires the negative-index materials used in the experiment must not have large absorption as well as defects, which is very difficult to achieve in existing fabrication techniques.[72] Another fascinating application of transformation optics is mimicking universal phenomena on optical chips. Sheng et al. experimentally demonstrated an optical analog of the effects of gravity on the motion of light rays, including light deflection and photon capture.[47] The "gravitational field" effect in their experiment is achieved by a microstructured waveguide spin-coated in the presence of a microsphere (Figure 2I), the refractive index distribution of which is similar to the form of gravitational field distribution around celestial bodies. Through this method, they also experimentally emulated the formation of Einstein's ring, which is a space-time curvature phenomenon predicted by Einstein's General Relativity.[73]

Although 3D metamaterials have been successfully used to solve many scientific issues and demonstrated exotic optical phenomena, it is still a big challenge to implement practical devices, due to the complex structures, large propagation loss, and high fabrication requirements.

3 | METASURFACE AND METALENS

In the past decade, ultrathin, ultralight, and high-efficiency metasurfaces have been widely studied, which are the 2D version of metamaterials and also possess powerful control abilities to EM waves. Different from the working principles of 3D metamaterials, the manipulation of EM waves by metasurface is through the interactions between the metaunit structure and the incident waves, resulting in abrupt light properties changes of the emergent light on the 2D plane. Compared with 3D metamaterials, metasurfaces are not only easier to be fabricated, but also avoid the propagation loss of light in bulk materials, so great attention has been received since they were first proposed by Capasso's group in 2011.[11] Capasso's group used Fermat's principle to derive that the reflective and refractive behavior of light on metasurfaces can be expressed by generalized Snell's law (Figure 3A):

$$\begin{cases} \sin(\theta_r) - \sin(\theta_i) = \dfrac{\lambda_0}{2\pi n_i}\dfrac{d\phi}{dx}, \\ \sin(\theta_t)n_t - \sin(\theta_i)n_i = \dfrac{\lambda_0}{2\pi}\dfrac{d\phi}{dx}. \end{cases} \quad (5)$$

Where λ_0 is the working wavelength, n_t and n_i are the refractive index of the medium on both sides of the interface, θ_i, θ_r, and θ_t are the angles of incidence, reflection, and transmission, respectively, $d\phi/dx$ is the gradient phase introduced by metasurface. According to generalized Snell's law, metasurfaces designed to satisfy specific phase gradients can refract light in any direction. On the other hand, if we look from the perspective of Huygens–Fresnel's principle, the metasurface units can be regarded as the secondary wavelet sources, the radiation fields from which interfere in space to form any desired light-field distribution.

There are two types of metasurfaces, working with different principles. First is the resonant metasurfaces, in which the abrupt phase change of EM waves is caused by resonances in unit structures, including plasmon resonance and dielectric resonance. However, the other is the nonresonant type, including geometric (or Pancharatnam–Berry [PB]) phase metasurfaces and propagation phase metasurfaces. Next, we will introduce these different types of metasurfaces in detail.

3.1 | Resonant metasurfaces

The early proposed metasurfaces mainly used plasmonic metal resonant units to control the light field. For example, Yu et al. designed a metasurface composed of V-shaped antennas (Figure 3B), the double resonance effect which guarantees the light control can cover the full phase modulation range in mid-infrared.[11] Similarly, metasurfaces composed of H-shaped antennas or SRRs have also been proposed to achieve arbitrary phase modulation, owning to the high order resonances in the unit structures.[80] In addition, Ni et al. applied the Babinet principle to design a metasurface with hole structures as the resonant units (Figure 3C), which can also control phase at will by setting appropriate parameters.[74] Although plasmonic resonant structures possess advantages of small size and strong EM field locality,[81,82] they suffer from serious loss problems, especially at optical frequency, which limits the performances of the metasurface-based devices. To improve the efficiency, low-loss dielectric Huygens' metasurfaces have been proposed (Figure 3D),[75] the high refractive index dielectric units which support strong EM resonance modes, known as Mie resonances.[83] Researchers have found that the dielectric units can generate electrical and magnetic resonances of comparable intensity and overlapping spectral. Kivshar's group proposed that by properly designing the unit parameters, metasurfaces with high transmittance can be realized.[22,75] However, the working bandwidth of resonant metasurface is narrow, as the modulation is very sensitive to the structural parameters, which also places high requirements for fabrication accuracy.

3.2 | Geometric phase metasurface

The geometric phase metasurfaces consist of anisotropic scattering units with uniform geometric parameters (Figure 3E), and the phase control is realized by changing the orientations of units. Hasman and other researchers found that when circularly polarized light is incident on a dipole antenna, the modulated light will partially convert into the opposite circular polarization with a phase change determined only by the orientation of the dipole antenna.[84–86] Soon after Zhang's group systematically described the method of obtaining gradient phase by rotated nanorods.[76] The modulated

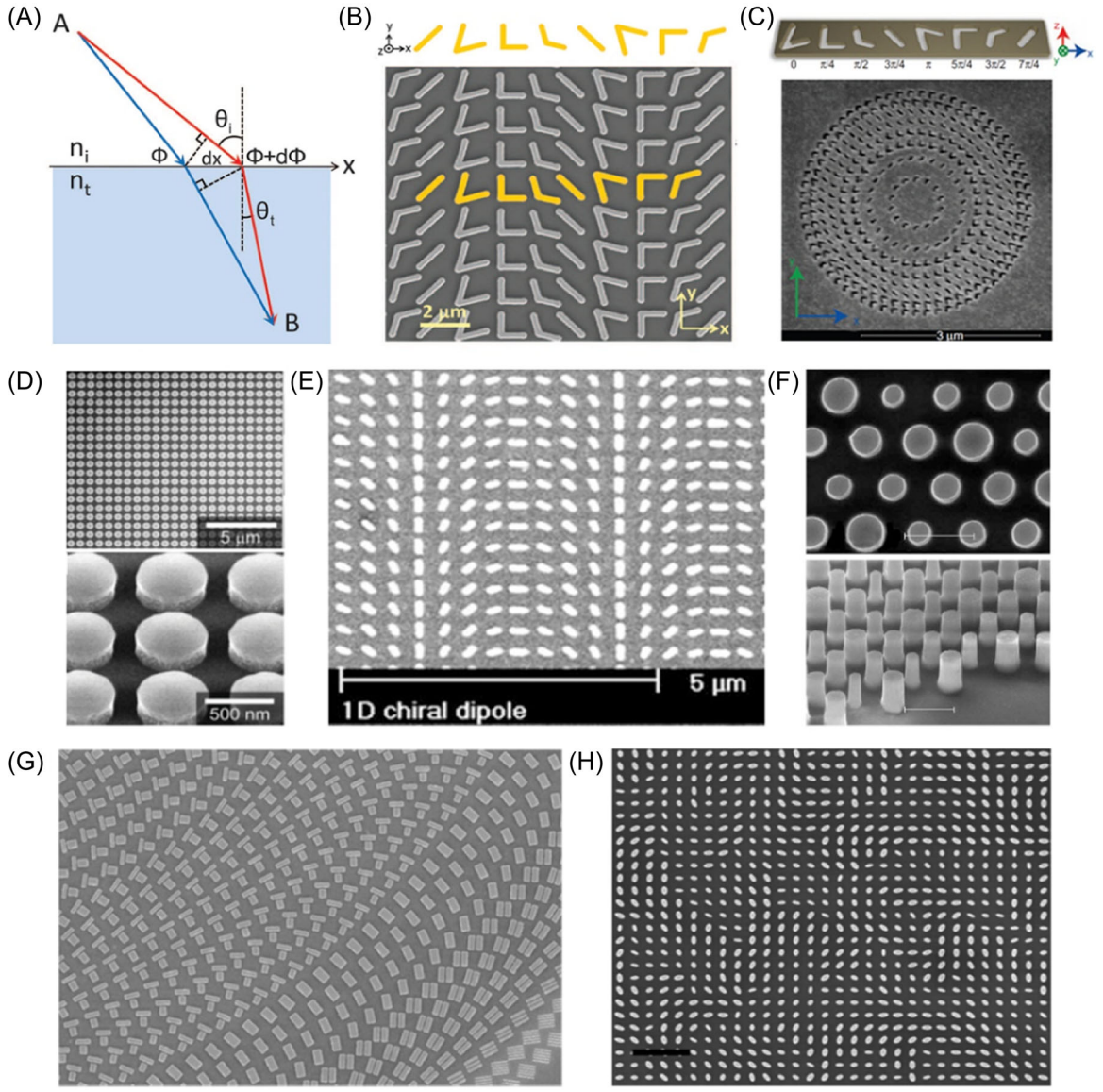

FIGURE 3 Various types of metasurfaces. (A) Schematic of the generalized Snell's law. Reproduced with permission.[11] Copyright 2011, American Association for the Advancement of Science. (B) Resonant metasurface is composed of V-shaped antennas. Reproduced with permission.[11] Copyright 2011, American Association for the Advancement of Science. (C) Babinet-inverted plasmonic metalens. Reproduced with permission.[74] Copyright 2013, Springer Nature. (D) High-efficiency dielectric Huygens' metasurface. Reproduced with permission.[75] Copyright 2015, WILEY-VCH. (E) The geometric phase metasurface. Reproduced with permission.[76] Copyright 2012, American Chemical Society. (F) Propagation phase metasurface. Reproduced with permission.[77] Copyright 2015, Springer Nature. (G) Broadband achromatic metalens with a combination of resonant phase and geometric phase. Reproduced with permission.[78] Copyright 2017, Springer Nature. (H) Multiplexed phase modulation under different polarizations is realized by a combination of geometric phase and propagation phase. Reproduced with permission,[79] Copyright 2017, American Physical Society.

transmission field under the normal incidence of circularly polarized light is found as

$$E_t = \hat{t}(\theta)|\sigma\rangle = \frac{t_o + t_e}{2}|\sigma\rangle + \frac{t_o - t_e}{2}e^{\mp i2\sigma\theta}|-\sigma\rangle, \quad (6)$$

where t_o and t_e are the complex transmission coefficients along the long and short axes of the nanorod, respectively, and $\sigma = 1/-1$ corresponds to left-handed/right-handed circular polarization. The first term on the right side of the equal sign in Equation (6) represents light with the same polarization as the incident light, while the second term is the orthogonal circularly polarized light with an extra phase of $\mp 2\sigma\theta$. This extra phase is the geometric phase, also known as the PB phase. According to this equation, if the nanorod is rotated from 0 to π rad, the phase control of orthogonal circularly polarized light will cover the full 2π range. Thanks to the simple unit

structure and wavelength-independent phase modulation mechanism, geometric phase metasurfaces have been widely used in recent years.[87–91] However, due to its design for circularly polarized light, additional polarizing and analyzing optical elements are required for high-quality light control, which inevitably reduces the light energy efficiency.

3.3 | Propagation phase metasurface

The units in this type of metasurface are dielectric nanoposts with a high aspect ratio, which can be regarded as truncated dielectric waveguides (Figure 3F). By changing the cross-section size, nanoposts will possess different effective propagation constants, resulting in required phase accumulation via propagation over the nanoposts.[92,93] Although high aspect ratio nanoposts place high fabrication requirements, such polarization-insensitive and high-efficient metasurfaces are of great use in practical applications. Faraon's group realized a series of metasurfaces-based devices by using high refractive index silicon nanoposts as the units.[77,94–98] In 2018, Dong's group achieved a metasurface of 80% transmittance in the visible regime, which is composed of silicon nitride nanoposts.[99]

Recently, strategies that combine two or more types of metasurfaces have been proposed to enrich the control functions and improve control performances. The V-shaped metal antennas proposed by Capasso's group in 2011 contain the modulations of the resonance phase and the geometric phase.[11] In the designed eight diffraction units, the first four are resonant units that realize phase modulation from 0 to π through different resonance modes. Then after rotating 90°, the latter four units can be obtained to cover the remaining π to 2π phase modulation range. Continuous broadband achromatic metalenses are another example that benefits from the combination of resonant phase and geometric phase (Figure 3G), which will be discussed later. Moreover, researchers have also studied the combination of geometric phase and propagation phase (Figure 3H), based on which they realized not only multiplexed phase modulation under different polarizations,[79] but also simultaneously independent control of amplitude, phase, and polarization.[100–102]

3.4 | Metalens

On the basis of different types of metasurfaces, rich functionalities have been implemented, among which metalens is the most concerned one due to the extremely wide applications in optical systems. Metalenses offer two major advantages in imaging technology.[103] First, the ultrathin, ultralight, and flat architectures favor minimization and compact devices. Second, their function multiplexing and expansion abilities provide flexible wavefront shaping, polarization control, and spectrum tailoring. Metalens can focus normally incident light into a point if a hyperbolic phase distribution is designed, expressed as

$$\varphi(r) = \frac{2\pi}{\lambda}\left(f - \sqrt{r^2 + f^2}\right), \tag{7}$$

where λ is the working wavelength, r is the radial position from the center, and f is the focal length. Early realized metalenses were composed of plasmonic nanostructures,[104–106] the large intrinsic losses which lead to low working efficiencies of metalenses. In 2016, Capasso's group proposed a TiO_2-based metalens with an efficiency of 86%,[107] the good imaging performance of which attracted much attention. Since then great efforts have been made by researchers to further improve the performances of metalenses, including efficiency, working bandwidth, and field of view (FOV).

Due to the diffractive optical properties of metalenses, they have obvious chromatic aberration without special design, which significantly limit their applications, especially in color imaging and display. To address this issue, achromatic metalenses working at several discrete wavelengths were achieved by integrating multiple lenses into the same platform.[108–114] Research further realized continuous broadband achromatic metalenses by optimization of metastructures.[115,116] Through this method, Capasso's group demonstrated a reflective achromatic metalens that have an invariant focal length from 490 to 550 nm.[115] By exploiting the geometric phase combined with phase compensation from well-designed integrated-resonant elements, Tsai and Li's joint group successively realized broadband achromatic metalenses in the near-infrared (Figure 4A) and the visible.[78,122,123] Capasso's group combined geometric phase and resonance phase within the nanofins to simultaneously control the phase and group delay dispersion, which also successfully resulted in broadband achromatic metalens in the visible (Figure 4B).[117]

The FOV is one of the key indicators of imaging systems, which is usually limited by off-axis aberration (especially coma aberration). In traditional large-FOV imaging systems, compound lenses with bulky thickness are used to eliminate coma aberrations. While for the ultimate goal of compact imaging, people are working for a singlet or few-layered metalenses to achieve the same function. Thus, in recent years, great efforts have been made to enlarge the FOV based on metalenses. However, a traditional single metalens still has a limited FOV, due to the fact that the focusing phase profile can hardly be

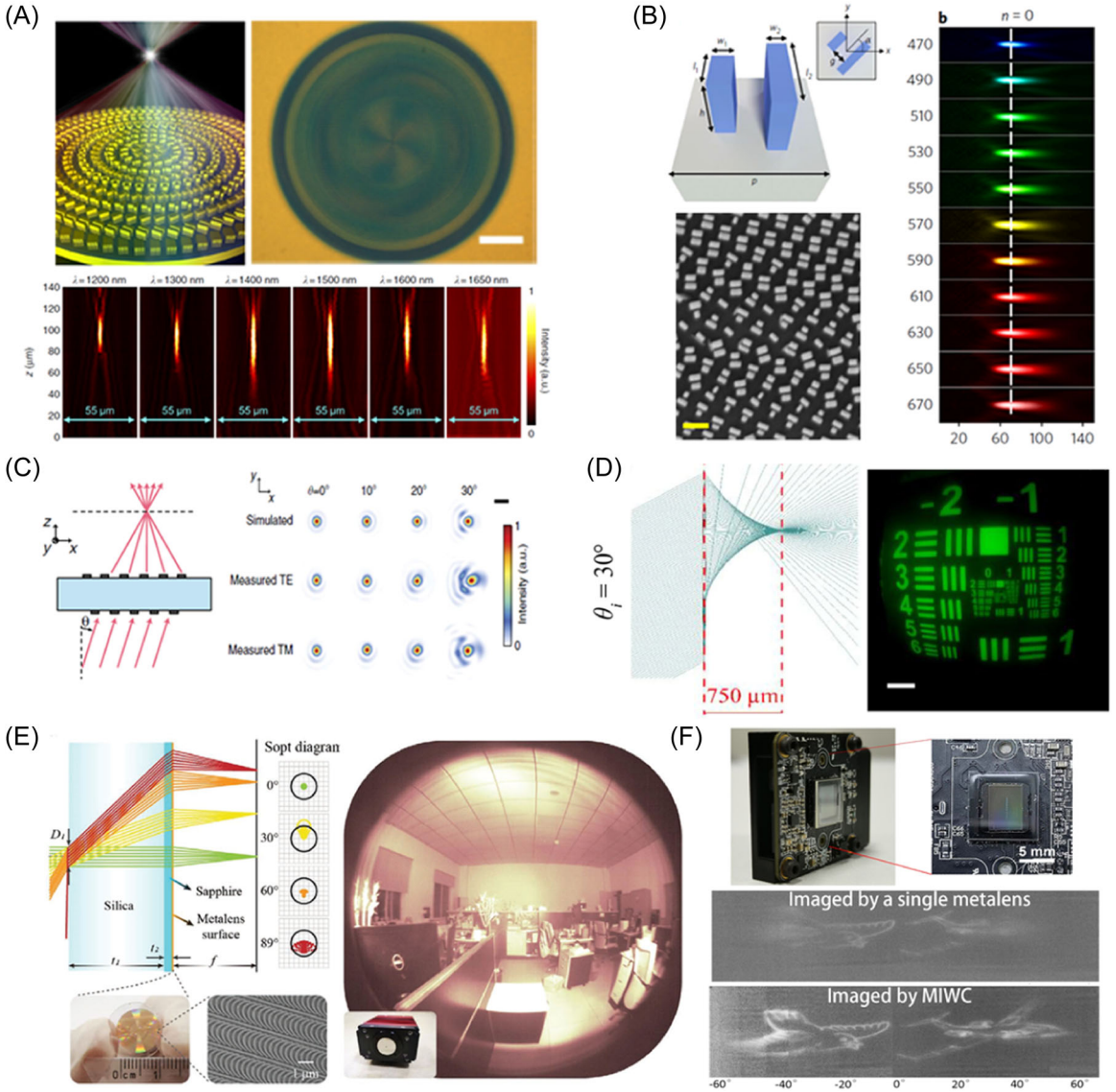

FIGURE 4 Metalenses. (A) Reflective achromatic metalens with 450 nm bandwidth in infrared. Reproduced with permission.[78] Copyright 2017, Springer Nature. (B) Transmissive achromatic metalens with 200 nm bandwidth in visible. Reproduced with permission.[117] Copyright 2018, Springer Nature. (C) Metalens doublet with a viewing angle of ±30°. Reproduced with permission.[118] Copyright 2016, Springer Nature. (D) Monolayer quadratic metalens with a viewing angle of ±70°. Reproduced with permission.[119] Copyright 2020, American Chemical Society. (E) Dielectric-gapped landscape quadratic metalens with a viewing angle near 180°. Reproduced with permission.[120] Copyright 2021, Wiley-VCH. (F) Metalens array-based wide-angle camera, which can realize high-quality imaging with a viewing angle as large as 120°.[121]

satisfied for all incident angles.[124] Recently, several types of metalens designed to enlarge FOV have been proposed, including optimized multiparametric geometries,[125,126] monolayer quadratic metalens (Figure 4D),[119,127,128] air-gapped landscape quadratic metalens,[129–131] dielectric-gapped landscape quadratic metalens (Figure 4E),[120] and metalens doublets (Figure 4C).[118,132] However, these methods either sacrifice imaging performances or imaging efficiencies. Li's group proposed a metalens array-based wide-angle solution, through which the angular focusing problem was transformed into the multiple distributions in the planar dimension. And they successfully realized high-quality imaging with a viewing angle as large as 120°, by a very compact meta device (Figure 4F).[121]

4 | META STRUCTURES DESIGN AND OPTIMIZATION

4.1 | Design through numerical simulations

Although there are clear physical models in classic metastructures, it is often difficult to analytically derive

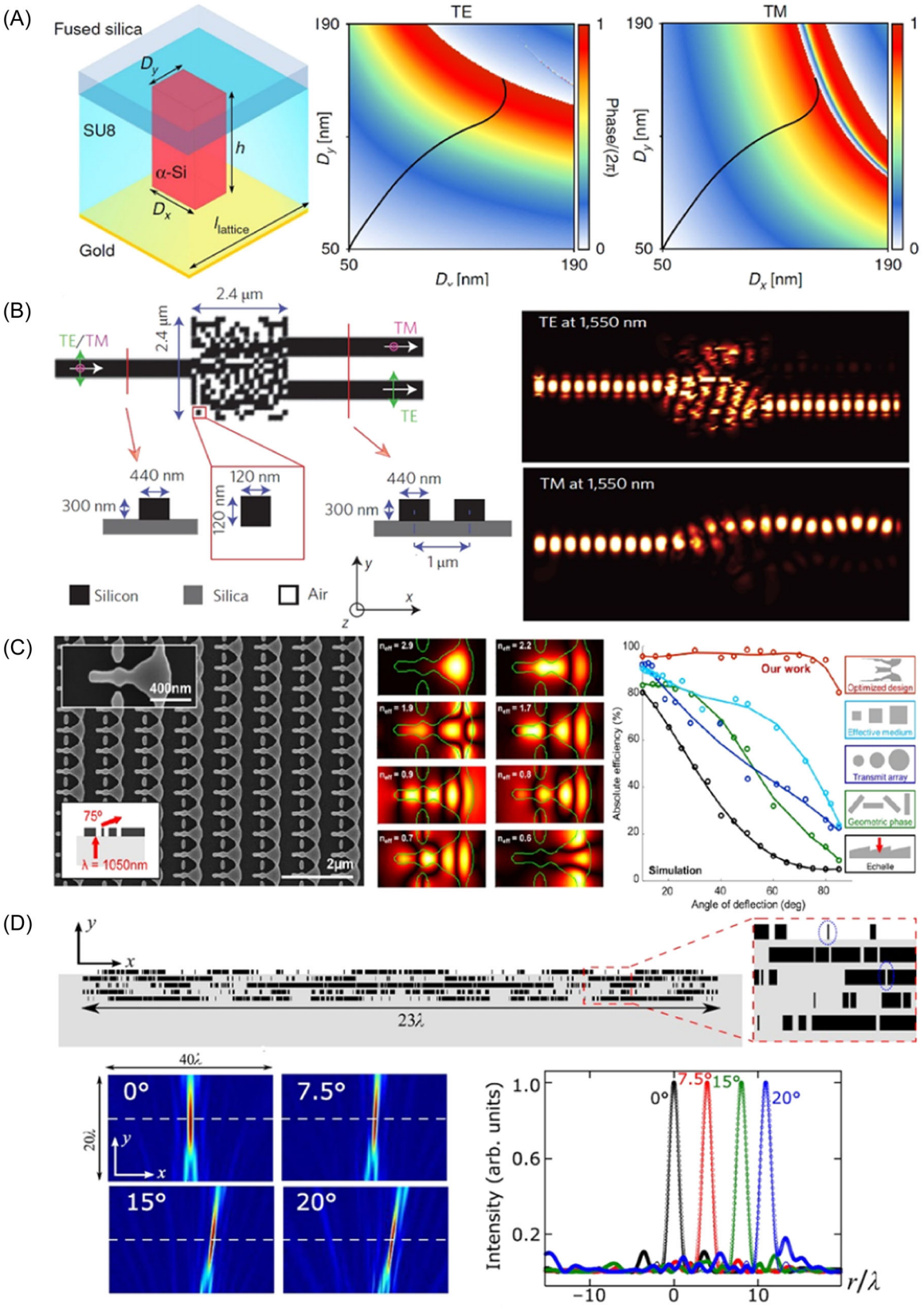

FIGURE 5 Metastructure simulation and optimization. (A) Schematic of a rectangular meta-atom capped by SU-8 polymer and the simulated phase maps plotted for transverse electric (TE) and transverse magnetic (TM) polarizations. Reproduced with permission.[94] Copyright 2018, Springer Nature. (B) Photonic beam splitter designed by the direct-binary search algorithm. Reproduced with permission.[134] Copyright 2015, Springer Nature. (C) Topology-optimized freeform metasurfaces for beam deflector with ultrahigh efficiency. Reproduced with permission.[135] Copyright 2017, American Chemical Society. (D) Multilayered 2D wide-angle metalens designed by a topology-optimized algorithm. Reproduced with permission.[125] Copyright 2018, American Physical Society.

the structure parameters, due to the complexity of the structure or the deviations from reality and ideal models. So in most metamaterial works, people retrieve the structure parameters from numerical simulations by using some commercial software, including Lumerical Finite-Difference Time-Domain (FDTD) solutions, COMSOL Multiphysics, CST Microwave Studio, ANSOFT, and so forth. With this software, people can construct the models of metastructures and simulate the optical responses under different parameters based on numerical algorithms, such as FDTD and Finite Element Method.[30,133] In early 3D metamaterials works, transmission and reflection of the composite metamaterials are first calculated by the simulation software, and then used to derive the permittivity and permeability. In metasurface design, generally, only a single unit model with periodic boundary conditions is simulated. Then the phase or transmission responses corresponding to different structure parameters are obtained from the simulated data library to guide the design of the entire metasurface device (Figure 5A).

4.2 | Inverse design by classical optimization techniques

For some classical functions, under the guidance of physical models, the metadevice can generally be designed by parametric sweeps in simulation software. However, if the device function is too complex, the construction units for metamaterials with the common physical model cannot meet the requirement, and the parametric sweeps will be insufficient. Complex, compound, or even random shapes of structures will probably work, the huge parameter space makes the parametric sweeps almost impossible to complete the structure design. In this section, we will introduce the inverse design methods, that is, find the parameters of a metasurface to exhibit the desired function with the assistance of optimization algorithms. The inverse design problem can be solved as an optimization problem that minimizes or maximize an objective function of the unit cell parameters subject to some constraints (Figure 5B).[29,31,134,136–139] The objective function is the mathematical expression of what functionality the metadevice is to achieve.

What kind of optimization algorithm is chosen for a particular metadevice design is of importance, since there is no single optimization algorithm that is perfectly suited for all problems. To choose the best optimization strategy, one needs to determine which category his design belongs to according to some questions. For example, is the input space discrete? If yes, that means there is a finite number of potential solutions to search from. In this condition, global optimizers like the Genetic Algorithm (GA) will be a good choice, for it is good at finding the optimal design from large solution spaces for noncontiguous structure.[140] But if the structure is contiguous, the Ant Colony Optimization algorithm will be better than GA.[141] Then for problems with continuous input space, there will be another question: Is it a finite element problem? If yes, the topology optimization method will be a good candidate. Topology optimization refers to the idea of optimizing a 2D or 3D system comprising an array of elements (Figure 5C,D), each of which contains parameters requiring adjustment.[125,135,142–144] Otherwise, a number of gradient-based algorithms can be used for optimization, including Newton's method[145] and the multiobjective Gradient Descent algorithm.[146] There are still other cases of problems and their corresponding suitable algorithms, detailed discussion seen in Campbell et al.[30]

We can see that these optimization algorithms are rule-based approaches containing iterative searching steps in a case-by-case manner. It is not friendly for inexperienced researchers to select the correct algorithms for different application scenes, which requires researchers to be familiar with the characteristics of each algorithm. In addition, these algorithms usually need a lot of computation sources including power and time and hence are insufficient for complex design while the dimension of parametric space and number of constraints increases.

5 | DESIGN METASTRUCTURES WITH AI ALGORITHMS

5.1 | Basic concepts

In recent years, as an important part of AI algorithms, data-driven machine learning algorithms have developed rapidly in the fields of industrial production, scientific research, medical diagnosis, economic analysis, and so on.[147] Machine learning algorithms establish links between input parameters and output results by looking for the laws in a large amount of data. This process is known as the learning or training process, which can constitute a mathematical model to connect the input and output data. Once the model is trained, it can be used to make predictions on unknown data, which looks like intelligent behaviors. When training or using the model, no physical or mathematical meaning of the specific problem needs to be understood, thus machine learning method is universal and can be used to solve various problems, including classification, regression, clustering, and structured prediction.[148–151] It should be noted that big data are of great importance

for the performance of machine learning methods. Generally, higher quality and a larger amount of data result in more accurate predictions. Usually, it takes a lot of time and effort to collect a large amount of data and train the model, but using the model is convenient and time-saving. So the machine learning method is more suitable for situations where the model needs to be used repeatedly after it is established.

In the past few decades, machine learning has developed many classical algorithms, including support vector machine, decision tree, Bayesian classifier, ANNs, and so forth. Among them, deep learning based on multilayer ANNs is one of the most popular machine learning methods, which has been successfully applied in autonomous driving, target recognition, machine translation, and speech recognition.[152–156] In a biological neural network, the basic unit is a neuron, which is connected to other neurons. If the electrical potential of a neuron exceeds a threshold, it will be activated and send chemicals to other connected neurons whose electrical potential thereby also be changed. ANN is a mathematical algorithm model that imitates the behavioral characteristics of biological neural networks and performs distributed parallel information processing. In an ANN model, each neuron receives input signals from other connected neurons. These input signals are transmitted through weighted connections to receive the total input value which will be then compared with the neuron's threshold and processed through an activation function to produce the neuron's output. An ANN consists of an input layer, an output layer, and more than one hidden layer. The neurons in the input layer receive external data, which then be processed through hidden layers and the output layer, and the final result is output by neurons in the output layer.[157,158] The training process of the neural network is using a large amount of data to continuously iterate the weights of connections between neurons with the help of methods, such as the error back-propagation (BP) algorithm until the output results from the neural network can be consistent with the ground truth. After training, the ANN can accurately map the input to the desired output.

5.2 | Neural network-assisted metadesigns

We can use ANN to establish relationships between the metamaterials structure parameters and the optical responses (Figure 6). The inverse process of the ANN is to derive the corresponding parameters from the target function, which can be applied for metastructure design. The forward process is also very useful, as it provides a simple mathematical way to obtain physical phenomena from structure parameters, which otherwise needed to be calculated by time-consuming FDTD or other simulation methods.

A representative example is using neural networks to design structures of core–shell metamaterial unit, which is composed of multilayers with different thicknesses and dielectric permittivity (Figure 7B). Peurifoy et al. first applied ANN to study the scattering properties of core–shell nanoparticles.[165] The inputs of the network are the thickness of the layers ranging from 30 to 70 nm and the outputs are the scattering spectrums in the wavelength range between 400 and 800 nm. After training, the ANN can generate the scattering spectrum for a given set of

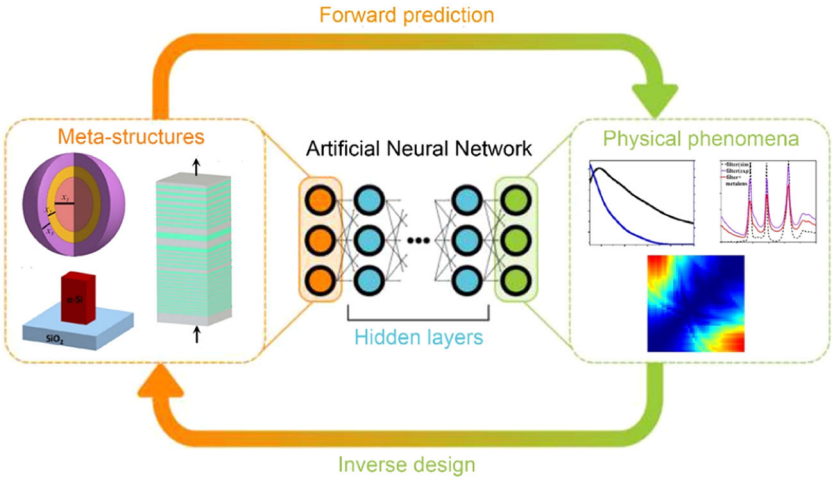

FIGURE 6 Neural network-assisted metadesigns. The ANN mathematically connects the metastructures and the physical phenomena. The inverse process can be applied for intelligent metadesigns from target functions. The forward process is useful for the quick prediction of physical responses from certain metastructures. ANN, artificial neural network.

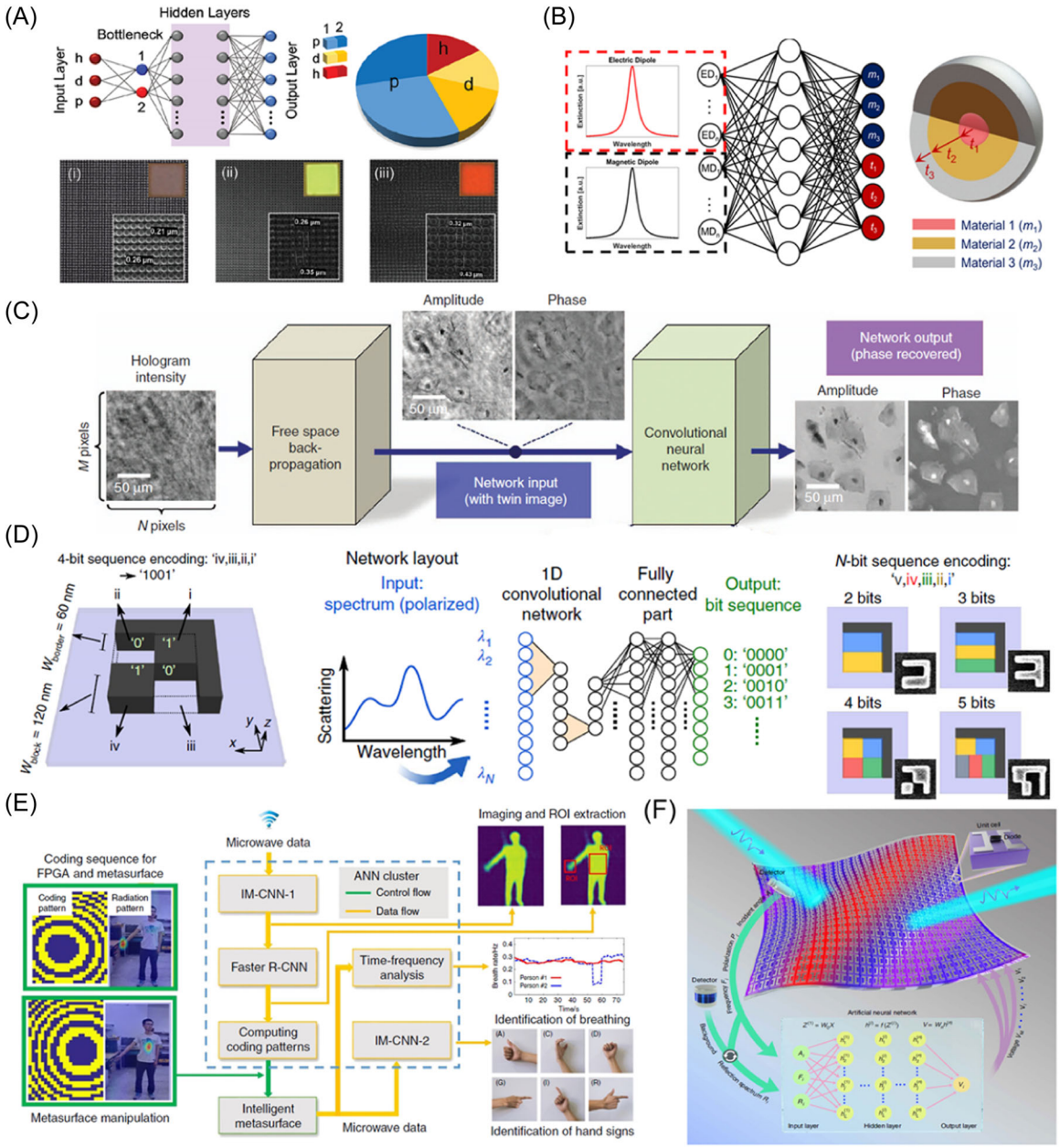

FIGURE 7 Intelligent meta-applications. (A) Full-color generation with HfO_2 metasurface designed by deep learning. Reproduced with permission.[159] Copyright 2019, Royal Society of Chemistry. (B) An ANN for studying the scattering properties of multilayer core–shell nanoparticles. Reproduced with permission.[160] Copyright 2019, American Chemical Society. (C) Phase recovery and holographic image reconstruction using a deep neural network. Reproduced with permission.[161] Copyright 2018, Springer Nature. (D) High-density planar optical information storage is enabled by deep learning. Reproduced with permission.[162] Copyright 2019, Springer Nature. (E) Programmable intelligent metasurface used for imaging and recognizing. Reproduced with permission.[163] Copyright 2019, Springer Nature. (F) Deep-learning-enabled self-adaptive microwave cloak without human intervention. Reproduced with permission.[164] Copyright 2020, Springer Nature.

parameters very precisely within a fraction of a second. In addition, the ANN can also be used as an inverse design tool, which determines the structure parameters from a target spectra. Hu et al. completed the same task with an improved ANN structure called a modified denoising autoencoder neural network.[166] A series of studies that supplement ANN with other methods were also proposed in the past 3 years to further improve the model performances.[160,167,168]

Apart from the research on nanoparticle scattering properties, more works focus on using ANNs to realize the overall functions of metadevices, including metalenses,

metaholograms, structural colors, and many other functions. Sometimes if the parameter space is too large, or the metastructures are difficult to parameterize, simple fully connected ANN will not work well. Therefore, in practical applications, some advanced ANNs models are used for metadevices design, such as convolutional neural networks (CNNs), recurrent neural networks, generative adversarial networks (GAN), and some improved networks based on these basic ones that are made according to specific problems. We would like to introduce several examples of metadevices benefiting from neural network approaches.

5.3 | Intelligent meta-applications

Starting from metalens, one of the most successful applications of metasurfaces. An et al. proposed a broadband achromatic metalens in the near-infrared design based on deep neural networks (DNN), which connect phases of metaunits and their geometric parameters. Two achromatic metalenses composed of elliptical nanopillars and nanofins were designed by the DNN and simulated, demonstrating the validity of their method.[169] Fan and Su combined different numbers of nanofins as the metalens unit and used DNN to train their data library. The well-trained model then predicted new data with the higher transmission, which could contribute to a broadband achromatic metalens in the visible with focusing efficiency as high as 45%.[170] Gu et al. designed a bifocal metalens that focuses the orthogonal polarization components of incident light to two independent spots. In their work, a DNN is trained to refine the unit cell simulation result of parameter sweep and benefits the efficient design of the metalens.[171] Zarei and Khavasi employed an inverse design method combining FDTD parameter sweep with Fourier-optics simulations, which performs like error BP in neural networks. Through this method, a number of thermally controlled varifocal metalens doublets and triplets were designed based on the thermo-optical effect of silicon.[172]

Holography is also an important application of metasurfaces, which can fully demonstrate the flexible phase control ability of metasurfaces. With the help of deep-learning methods, researchers have successfully improved the imaging quality, imaging speed, and imaging efficiency of metasurface holography. Ozcan's group demonstrated that a CNN can perform phase recovery and holographic image reconstruction after training. Compared with existing holographic phase recovery approaches, the deep-learning-based technique they employed is faster to compute and reconstruct high-quality images of objects by eliminating twin-image and self-interference-related artifacts (Figure 7C).[161] On the basis of this achievement, 2 years later their group used a GAN to perform cross-modality image transformation from a digitally BP hologram into a speckle- and artifact-free bright-field microscopy image.[173] This deep-learning-enabled holographic microscopy enables the reconstruction of volumetric samples from a single-hologram measurement without any mechanical scanning. Gu's group used a multilayer ANN to statistically learn the relationship between a given 3D vectorial field in the image space and the 2D vector field distribution in the hologram plane. And they successfully demonstrate 3D vectorial holography for the time-efficient and accurate reconstruction of 3D vectorial holographic images.[174] Cui's group proposed an efficient noniterative algorithm for designing metasurface holograms by a deep-learning structure composed of unsupervised variational autoencoder (VAE) and conditional generative adversarial networks (cGANs). The usage of unsupervised VAE structure makes their system easily trained from scratch and the noniterative structure of the generator in cGANs enables the realization of holographic imaging with high quality and high efficiency.[175] Ma et al. proposed and experimentally demonstrated the application of statistical machine learning in the design and optimization of complex multifunctional metasurfaces.[176] They successfully realized metasurface focusing lenses and holograms, which showed up to eight controllable functionalities for different combinations of working frequencies and polarization states, far beyond the design capability of traditional approaches. Besides, researchers have also used deep-learning methods to achieve metasurface holograms with complex functions or high performances, such as multicolor holograms[177] and high-efficiency holograms.[178]

Structural colors based on absorbing or scattering of light in metasurfaces may be widely used for digital displays, cryptography, optical data storage, security, and many other applications.[179,180] The deep-learning method will be a powerful tool to minimize the computation cost and maximize the design efficiency for structural color design. Yu's group trained a bidirectional DNN, the forward modeling process which can accurately predict the color generated by random silicon nanostructures, while the inverse design process which can accurately output the device geometries for at least one million different colors.[181] Hemmatyar et al. used a deep-learning algorithm based on a dimensionality reduction technique to design and optimize dielectric metasurfaces consisting of a square-lattice array of hafnia nanopillars and generated vivid and pure structural color with a wide color gamut (Figure 7A).[159] Rho's group employed a reinforcement learning method called *Q*-learning for optimization of color generation from dielectric nanostructures. The model is capable of finding

the best possible solution in millions of choices without ever experiencing it, thus helping the authors to find geometrical properties from a possible 34.5 million solutions that can generate much purer red, green, and blue colors compared with other reported results.[182] Macias' group proposed a metamodel-based optimization scheme that combines ANNs and a particle swarm optimization to tailor the chromatic response of periodic metastructures, including one-dimensional gratings[183] and arrays of nanoparticles with arbitrary cross-section,[184] and experimentally reproduced arbitrarily prescribed colors from the employed model. In addition, there are multiple other works using deep learning to efficiently design structural colors in plasmonic and metamaterial structures.[185–187]

Other practical metasurfaces applications designed by intelligent algorithms include light sails,[188,189] optical information storage (Figure 7D),[162] perfect absorbers,[190] biosensors,[191–194] and energy conversions.[195] In these metasurface designs, intelligent algorithms perform not only faster, but also more powerful than traditional methods. On the one hand, intelligent algorithms allow a much larger parameter space for optimization, which increases the probability of finding the optimal solution. On the other hand, intelligent algorithms establish special correlations between metasurfaces structures and physical phenomena, which are difficult to be represented by physical models or mathematical expressions. Most of the introduced metadevices above are for specific application scenarios, as the structures are fixed after design. Besides, there are some works that applied dynamically reconfigurable metamaterials. With the assistance of intelligent algorithms, the metastructures can make adaptive adjustments according to external environment changes or functions switch, which look more like an intelligent device. These metamaterials are often termed digital metamaterials or programmable metamaterials, which we will discuss below.

5.4 | Reconfigurable metamaterials with self-adaptive properties

Recently the concept of digital metamaterials has been proposed,[196,197] the constitutive 1-bit meta-atom is digitalized as "0" or "1" corresponding to two opposite EM responses. By incorporating an electric diode into the unit cell of metamaterials, the scattering state can be controlled by applying different biased voltages across the diode. When the digital meta-atom is programmable, a metamaterial can be used to realize different functions when programmed with different coding sequences via the field programmable gate array (FPGA). Moreover, as the states of programmable meta-atoms can be quickly switched, it enables the information coding and processing on the physical level of metamaterials in real-time.[198] Intelligent algorithms are extremely useful for realizing self-adaptive programmable metamaterials, for the reason that they can be used as a quick feedback mechanism, redefining programming sequences of the programmable metamaterials to adjust to environmental changes. Li et al. combined machine learning techniques with a 2-bit digital metasurface to realize a microwave reprogrammable imager. After a period of training, the proposed microwave imager can directly produce high-quality imaging and high-accuracy object recognition without the need for costly computational image reconstruction.[199] They also used an integrated network composed of three ANNs to simultaneously realize a smart metasurface imager and recognizer. The network they trained can transform measured microwave data into images of the whole human body, classify specifically designated spots within the image and recognize human hand signs instantly at a Wi-Fi frequency of 2.4 GHz (Figure 7E).[163]

In the field of wireless communications, intelligent reflecting surfaces (IRSs) recently have received much interest in the academia and industry for they are promising in next-generation (i.e., 6G) communications to achieve faster and more reliable data transmissions.[200,201] IRS comprises an array of reflective units, each of which can independently incur some change to the incident signal, such as the phase, amplitude, frequency, or polarization, without consuming transmit power. In essence, an IRS intelligently configures the wireless environment to help the transmission between the sender and receiver, when direct communications have bad qualities. Liaskos et al. used deep learning for configuring IRS to aid wireless communications. Specifically, wireless propagation is regarded as a neural network in their work, where IRS units are neurons and their cross-interactions are links. The trained network could learn the propagation basics of IRS and configures them to the optimal setting.[202] Taha et al. trained an ANN using only IRS units connected to the baseband of the IRS controller, which was then used for channel estimation in IRS communications and guiding the IRS to learn the optimal interaction with the incident signals.[203]

In recent years, research has tried to endow invisibility cloaks with intelligence, independence, and self-adaptability. Chen's group applied deep-learning algorithms into an invisibility cloak and built an intelligent cloak that exhibited a millisecond response time to an everchanging incident wave and the surrounding environment without any human intervention (Figure 7F).[164] The reconfigurable metasurface they used is composed of varactor diodes, the reflection

spectrum of which can be dynamically altered by feeding different bias voltages across it. Incoming waves sensed by detectors in real-time are processed by the ANN to calculate voltages, which then will be applied across the diodes to adjust the scattering spectrum and thus produce a scattered wave similar to that generated by the bare surrounding without a hidden object.

6 | DISCUSSIONS AND PERSPECTIVES

After more than 10 years of development, metamaterials research has undergone a series of changes from physical phenomenon demonstration to devices development, from exploring principles to improving devices performances, from single function to multifunctional integration, and from conventional design to intelligent design. Although the working principles of metamaterials have been well studied and based on which many practical applications have been realized, there are still some key scientific issues and technical bottlenecks waiting to be solved and overcome especially in metasurfaces applications. In this section, we will comment on some directions, challenges, and perspectives of metamaterial research.

6.1 | Full control of metamaterial angular dispersions

A key scientific problem that currently restricts metalens and related metadevices is the uncontrollability of their phase distributions to incident EM waves at different angles. It is a very important issue in metalens aberration correction and wide working angle metadevices. Although some angular dispersion has been manipulated by coupling effect[204] or tilting units,[205] the control abilities and performances are still far from arbitrary angular control. In particular, the problem of low modulation efficiency to large-angle incident light has not been well solved in principle, which will be the bottleneck in realizing high-efficiency wide-angle metadevices.

6.2 | Constraints among metasurface frequency dispersion, phase distribution, and working efficiency

In achromatic metadesigns, the large diffractive dispersion needs to be compensated by the constituting nanostructures, which mainly depends on the propagation phase in the transmission scheme. The required phase compensation would be huge as the achromatic lens size increases. Since the lateral parameters of nanostructures cannot change so large in very limited unit cells, to access a large compensation phase these nanoposts need to have a very large height with a large aspect ratio that undoubtedly adds great challenges to nanofabrication. In fact, there have been several papers concerning on the issue, and the relation between the maximum radius of the ideal achromatic lens was derived approximately as[206]

$$R \le \omega_c \frac{H\Delta n}{\Delta\omega} \frac{NA}{1-\sqrt{1-NA^2}}. \tag{8}$$

From Equation (8) we may find the $R_{\max}$ only has a positive relationship with the height (H) of nanoposts, while is inverse to the bandwidth ($\Delta\omega$) and NA. This relation is also valid for another kind of flat lens—multilevel diffractive lens (MDL), which can be regarded as a paralleled strategy for an achromatic flat lens.[207] Different from metalens, the MDL stemmed from the diffractive optics with optimized complex ring heights, where sufficient phase compensation against the material and diffractive dispersion can be properly achieved. There have been a number of achromatic MDL reports showing relatively larger lens diameters compared with metalens thanks to its higher thickness, though it may have some flaws in angular dispersion and efficiency. Undoubtedly, there is still improvement space by further increasing the thickness with structural optimizations.

6.3 | Active control of metamaterials in the optical regime

Controlling the optical properties of metamaterials actively in real-time could take their functionalities to the next level and expand the boundaries of fundamental optical science.[208] In the millimeter-wave and microwave regime, varactor diodes have been successfully utilized to constitute reconfigurable metasurfaces, which can accomplish various functions dynamically via FPGA.[196] However, this kind of diode is no longer applicable in the visible and near-infrared, researchers have proposed a series of other means to achieve dynamic control function either by tuning the metamaterial's dielectric permittivity or changing its topology. One way to tune a metamaterial's properties in real-time is reconfiguring the physical shape or arrangement of its nanoantennas through micro-electro-mechanical systems, with which a varifocal metalens is realized with a switching speed on the order of kHz to MHz.[209] Liu's group realized dynamic generation of programmable images by integrating metamaterials with LCs,[210] which

can also be used for real-time scanning and 3D imaging. By using metamaterials fabricated on top of phase-change materials, large amplitude and phase changes will be achieved under a thermal or electrical impulse.[211] Through this method, dynamical metasurface beam-steering and reconfigurable diffraction-limited metalenses have been realized.[212,213] Besides electrical control is a more widely used technique to tune a material's optical properties. Transparent conducting oxides materials enable strong modulation of their optical properties under an applied bias, with which Park et al. achieved wide-angle beam steering with independent control of phase and amplitude.[214] The above-mentioned methods successfully realized active control of metamaterials in specific functions. Active metamaterials with high switch speed (GHz to THz), high reliability, and the ability that each pixel is controllable, still remain to be studied, which are of great significance in optical communications, light detection and ranging (LIDAR) and 3D imaging devices, such as augmented and virtual reality.

6.4 | Fabrication of large-scale metamaterial devices

Since the structure size of each metamaterial unit is on the scale of tens of nanometers, it usually requires trillions of units to build a macroscopic metadevice, and each unit also has multiple structural parameters. Therefore, if all the parameters of the units do not have repeatability or regularity, the parameters that need to be input in the fabrication process will reach the order of Tbit. Although there are some data compression methods, to achieve universal large-area fabrication, data import and export will be a huge challenge. At the same time, it is also a huge challenge to ensure the accuracy and uniformity of each unit on such a scale, as well as the stability of the fabrication equipment. Recent studies have shown that the higher performance of metasurfaces will lead to larger aspect ratio nanopillar structural units (such as 100:1), which is also a huge challenge for current micro–nano fabrication technology.

6.5 | Intelligent optimization of large-scale metamaterials

Similar to the problem in the fabrication of large-scale metamaterial, when the metamaterial size increases, the number of structural parameters will explode.One challenge is that a training set with a large amount of data is needed to be produced first, which is time-consuming through FDTD simulations or experimental characterizations. Another challenge is that the large solution space will make it difficult for even a very complicated neural network to learn the intrinsic relationship between metastructures and the physical responses.[215] New approaches that extend beyond standard deep-learning methods are required for large-scale metamaterial design. One possible way to address this problem is to use unsupervised or semisupervised learning methods. They require only a small number of labels and usually serve as tools for data clustering and dimensionality reduction, which could remarkably reduce the time consumption for preparing training data.[216,217] Using the insights from physics as a model prior to deep learning is also an effective way when the amount of training data is limited. Different from the nonphysical applications, metamaterial designing is governed by certain physical laws or models, which if applied to deep learning, the training data and network parameters are not wasted on "learning the physics." This will undoubtedly not only simplify the deep-learning model but also skip the collection of a large amount of data.[218–220]

6.6 | Optical ANNs enabled by metamaterials

Besides employing intelligent algorithms for nanophotonics design as we have discussed above, another meaningful combination of intelligent algorithms and nanophotonics is constructing photonic neural networks that could emulate the structural and functional features of biological neural networks. As the photon is an important information carrier exhibiting a broad bandwidth and low transmission scattering compared with electrons, the development of ANNs based on nanophotonics devices will achieve orders-of-magnitude improvements in both computational speed and energy consumption over existing solutions based on electronics.[221] In recent years, a variety of ways to implement optical neural networks have been proposed, such as ANNs based on layers of diffractive materials in free space (Figure 8A)[222,226] and ANNs based on photonic circuits on a chip.[227,228] As a kind of flexible diffractive material, metasurfaces or 3D metamaterials are very suitable for implementing the first kind of optical ANNs. Luo et al. realized a polarization-multiplexed metasurface-based optical neural network that can perform various complex object recognition tasks.[229] The intelligent device they proposed is composed of one layer of metasurface integrated into a complementary metal-oxide semiconductor (CMOS) imaging sensor, which can mimic an ANN with a single hidden layer. Gu's group fabricated multilayer diffractive metastructures by 3D nanoprinting which were also

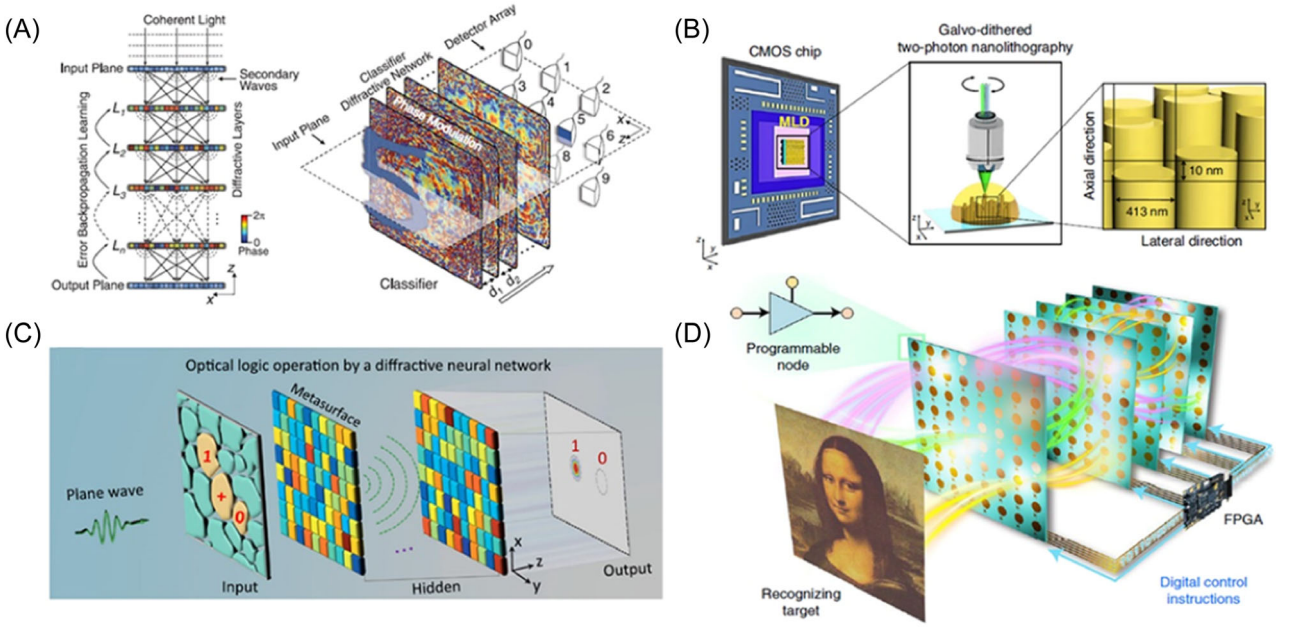

FIGURE 8 Metamaterials-based optical neural network. (A) Multilayer diffractive deep neural network for classifying and imaging. Reproduced with permission.[222] Copyright 2018, American Association for the Advancement of Science. (B) Machine learning decryptor integrated with a CMOS sensor. Reproduced with permission.[223] Copyright 2021, Springer Nature. (C) Schematic illustration of optical logic operations by a diffractive neural network. Reproduced with permission.[224] Copyright 2020, Springer Nature. (D) A programmable diffractive deep neural network platform able to handle various intelligent tasks. Reproduced with permission.[225] Copyright 2022, Springer Nature. CMOS, complementary metal-oxide semiconductor.

integrated on a CMOS chip (Figure 8B). Their experimental results demonstrated the application of their device as power-efficient optical decryptors and secure functional displays.[223] Chen's group used the compound Huygens' metasurface to construct a diffractive neural network and realized all seven basic types of optical logic operations in a compact system (Figure 8C).[224] The above-mentioned metasurfaces-based optical neural networks are all passive ones that are once these devices are fabricated only a fixed intelligent task can be performed. Cui's group applied their digital-coding metasurfaces technique to constructing a programmable diffractive DNN which they termed a programmable AI machine (Figure 8D).[225] This intelligent machine can handle various deep-learning tasks for wave sensing, including image classification, mobile communication coding, and real-time multibeam focusing fully showing what the next-generation of intelligent materials will look like. Although a series of inspiring results have been achieved on metastructures-based optical neural networks, there is still room for improvement. One key issue is the realization of the optical nonlinear activation function, which can endow optical neural networks with certain computational power for better performances in learning and predicting. Some previously reported optical neural networks lack the nonlinear activation part, which leads to their poor performances and limited functionalities. In recent years, research has proposed several methods for the realization of optical nonlinear activation functions such as laser-cooled atom with electromagnetically induced transparency[230] or using nonlinear materials, including crystals, polymers, or semiconductors.[231] However, how can these methods be combined with multilayer metasurfaces, especially dynamically tunable ones in the optical regime, still requires a lot of researches.

6.7 | Metasurfaces integrated with other nanostructures

Owning to the excellent flexibility in light-field manipulation, metasurfaces have been combined with other materials or nanostructures to realize ultracompact devices with high performances. For example, researchers fabricated hybrid metasurfaces by combining plasmonic nanostructures with transition metal dichalcogenides (TMDCs), such as WS_2, which can simultaneously enhance and manipulate the nonlinear processes in TMDC, facilitating nonlinear valleytronic nanodevices.[232–234] Li et al. integrated a metalens array with a nonlinear crystal, and demonstrated a 100-path spontaneous parametric down-conversion photon-pair source in a 10×10 array, indicating a new platform for integrated quantum devices.[235] Xie et al. realized monolithic integration of dielectric metasurfaces with vertical-cavity surface-emitting lasers that enable

arbitrary control of the laser beam profiles with high efficiency.[236] This function can be implemented in various wide-field applications, such as optical fiber communications, laser printing, face recognition, and ultracompact LIDAR.

In conclusion, the current metamaterial research has progressed from the initial study of the EM response of nanostructures and the simple control of the optical field to the development of photonics devices with specific functionalities and performance enhancement. As a large number of metamaterials-based works have been demonstrated, the bottleneck problems encountered in practical applications have gradually become prominent and attracted researchers' attentions. However, with the continuous progress of new design methods, new material systems, and fabrication technologies, we believe that the key problems discussed above can be further solved. Especially with the utilization of AI photonics technologies, many fundamental problems in hardware can be alleviated by sophisticated algorithms, which also bring excellent performances to the new generation of metamaterials-based photonic devices.

ACKNOWLEDGMENTS

This study is supported by the National Key R&D Program of China (2016YFA0202103), the National Natural Science Foundation of China (Nos. 12104223 and 91850204), and the Fundamental Research Funds for the Central Universities (Nos. 2242022R10128 and 2242022k30006). Tao Li thanks the support from Dengfeng Project B of Nanjing University.

CONFLICT OF INTEREST

The authors declare no conflict of interest.

ORCID

Ji Chen http://orcid.org/0000-0002-9376-6077
Shanshan Hu http://orcid.org/0000-0002-0174-1156
Shining Zhu http://orcid.org/0000-0002-3472-6497
Tao Li http://orcid.org/0000-0003-0049-471X

REFERENCES

[1] Engheta N, Ziolkowski RW. *Metamaterials: Physics and Engineering Explorations*. John Wiley & Sons; 2006.
[2] Cai W, Shalaev V, Paul DK. Optical metamaterials: fundamentals and applications. *Phys Today*. 2010;63(9):57-58.
[3] Smith DR, Pendry JB, Wiltshire MCK. Metamaterials and negative refractive index. *Science*. 2004;305(5685):788-792.
[4] Ramakrishna SA. Physics of negative refractive index materials. *Rep Prog Phys*. 2005;68(2):449-521.
[5] Fang N, Xi D, Xu J, et al. Ultrasonic metamaterials with negative modulus. *Nat Mater*. 2006;5(6):452-456.
[6] Fok L, Ambati M, Zhang X. Acoustic metamaterials. *MRS Bull*. 2008;33(10):931-934.
[7] Liu Y, Zhang X. Metamaterials: a new frontier of science and technology. *Chem Soc Rev*. 2011;40(5):2494-2507.
[8] Zheludev NI, Kivshar YS. From metamaterials to metadevices. *Nat Mater*. 2012;11(11):917-924.
[9] Jackson JD. *Classical electrodynamics*. Wiley; 1999.
[10] Veselago VG. The electrodynamics of substance with simultaneously negative values of ε and μ. *Sov Phys Usp*. 1968;10(4):509-514.
[11] Yu N, Genevet P, Kats MA, et al. Light propagation with phase discontinuities: generalized laws of reflection and refraction. *Science*. 2011;334(6054):333-337.
[12] Yu N, Capasso F. Flat optics with designer metasurfaces. *Nat Mater*. 2014;13(2):139-150.
[13] Genevet P, Capasso F, Aieta F, Khorasaninejad M, Devlin R. Recent advances in planar optics: from plasmonic to dielectric metasurfaces. *Optica*. 2017;4(1):139-152.
[14] Kruk S, Kivshar Y. Functional meta-optics and nanophotonics governed by Mie resonances. *ACS Photonics*. 2017;4(11):2638-2649.
[15] Aieta F, Genevet P, Kats MA, et al. Aberration-free ultrathin flat lenses and axicons at telecom wavelengths based on plasmonic metasurfaces. *Nano Lett*. 2012;12(9):4932-4936.
[16] Liu Z, Li Z, Liu Z, et al. High-performance broadband circularly polarized beam deflector by mirror effect of multinanorod metasurfaces. *Adv Funct Mater*. 2015;25(34):5428-5434.
[17] Bao Y, Yu Y, Xu H, et al. Full-colour nanoprint-hologram synchronous metasurface with arbitrary hue-saturation-brightness control. *Light Sci Appl*. 2019;8(1):1-10.
[18] Liang H, Martins A, Borges BHV, et al. High performance metalenses: numerical aperture, aberrations, chromaticity, and trade-offs. *Optica*. 2019;6(12):1461-1470.
[19] Lee D, Gwak J, Badloe T, Palomba S, Rho J. Metasurfaces-based imaging and applications: from miniaturized optical components to functional imaging platforms. *Nanoscale Adv*. 2020;2(2):605-625.
[20] Chen WT, Zhu AY, Capasso F. Flat optics with dispersion-engineered metasurfaces. *Nat Rev Mater*. 2020;5(8):604-620.
[21] Ni X, Wong ZJ, Mrejen M, Wang Y, Zhang X. An ultrathin invisibility skin cloak for visible light. *Science*. 2015;349(6254):1310-1314.
[22] Wang L, Kruk S, Tang H, et al. Grayscale transparent metasurface holograms. *Optica*. 2016;3(12):1504-1505.
[23] Totero Gongora JS, Miroshnichenko AE, Kivshar YS, Fratalocchi A. Anapole nanolasers for mode-locking and ultrafast pulse generation. *Nat Commun*. 2017;8(1):1-9.
[24] Khorasaninejad M, Capasso F. Metalenses: versatile multifunctional photonic components. *Science*. 2017;358(6367):eaam8100.
[25] Lalanne P, Chavel P. Metalenses at visible wavelengths: past, present, perspectives. *Laser Photon Rev*. 2017;11(3):1600295.
[26] Tittl A, Leitis A, Liu M, et al. Imaging-based molecular barcoding with pixelated dielectric metasurfaces. *Science*. 2018;360(6393):1105-1109.
[27] Krasnok A, Tymchenko M, Alù A. Nonlinear metasurfaces: a paradigm shift in nonlinear optics. *Mater Today*. 2018;21(1):8-21.
[28] Yesilkoy F, Arvelo ER, Jahani Y, et al. Ultrasensitive hyperspectral imaging and biodetection enabled by dielectric metasurfaces. *Nat Photonics*. 2019;13(6):390-396.

[29] Molesky S, Lin Z, Piggott AY, Jin W, Vucković J, Rodriguez AW. Inverse design in nanophotonics. *Nat Photonics*. 2018;12(11):659-670.
[30] Campbell SD, Sell D, Jenkins RP, Whiting EB, Fan JA, Werner DH. Review of numerical optimization techniques for meta-device design. *Opt Mater Express*. 2019;9(4):1842-1863.
[31] Li W, Meng F, Chen Y, Li Yf, Huang X. Topology optimization of photonic and phononic crystals and metamaterials: a review. *Adv Theory Simul*. 2019;2(7):1900017.
[32] Ma W, Liu Z, Kudyshev ZA, Boltasseva A, Cai W, Liu Y. Deep learning for the design of photonic structures. *Nat Photonics*. 2021;15(2):77-90.
[33] Ma L, Li J, Liu Z, et al. Intelligent algorithms: new avenues for designing nanophotonic devices. *Chin Opt Lett*. 2021;19(1):11301.
[34] Krasikov S, Tranter A, Bogdanov A, Kivshar Y. Intelligent metaphotonics empowered by machine learning. *Opto-Electron Adv*. 2022;5(3):210124-210147. doi:10.29026/oea.2022.210147
[35] Katsarakis N, Koschny T, Kafesaki M, Economou EN, Soukoulis CM. Electric coupling to the magnetic resonance of split ring resonators. *Appl Phys Lett*. 2004;84(15):2943-2945.
[36] Baena JD, Bonache J, Martin F, et al. Equivalent-circuit models for split-ring resonators and complementary split-ring resonators coupled to planar transmission lines. *IEEE Trans Microwave Theory Tech*. 2005;53(4):1451-1461.
[37] Zhou J, Koschny T, Kafesaki M, Economou EN, Pendry JB, Soukoulis CM. Saturation of the magnetic response of split-ring resonators at optical frequencies. *Phys Rev Lett*. 2005;95(22):223902.
[38] Aydin K, Bulu I, Guven K, Kafesaki M, Soukoulis CM, Ozbay E. Investigation of magnetic resonances for different split-ring resonator parameters and designs. *New J Phys*. 2005;7(1):168.
[39] Pendry JB, Holden AJ, Robbins DJ, Stewart WJ. Magnetism from conductors and enhanced nonlinear phenomena. *IEEE Trans Microwave Theory Tech*. 1999;47(11):2075-2084.
[40] Pendry JB, Holden AJ, Stewart WJ, Youngs I. Extremely low frequency plasmons in metallic mesostructures. *Phys Rev Lett*. 1996;76(25):4773-4776.
[41] Shelby RA, Smith DR, Schultz S. Experimental verification of a negative index of refraction. *Science*. 2001;292(5514):77-79.
[42] Fang N, Lee H, Sun C, Zhang X. Sub-diffraction-limited optical imaging with a silver superlens. *Science*. 2005;308(5721):534-537.
[43] Liu Z, Lee H, Xiong Y, Sun C, Zhang X. Far-field optical hyperlens magnifying sub-diffraction-limited objects. *Science*. 2007;315(5819):1686.
[44] Pendry JB, Schurig D, Smith DR. Controlling electromagnetic fields. *Science*. 2006;312(5781):1780-1782.
[45] Schurig D, Mock JJ, Justice BJ, et al. Metamaterial electromagnetic cloak at microwave frequencies. *Science*. 2006;314(5801):977-980.
[46] Lai Y, Ng J, Chen H, et al. Illusion optics: the optical transformation of an object into another object. *Phys Rev Lett*. 2009;102(25):253902.
[47] Sheng C, Liu H, Wang Y, Zhu SN, Genov DA. Trapping light by mimicking gravitational lensing. *Nat Photonics*. 2013;7(11):902-906.
[48] Smith DR, Padilla WJ, Vier DC, Nemat-Nasser SC, Schultz S. Composite medium with simultaneously negative permeability and permittivity. *Phys Rev Lett*. 2000;84(18):4184-4187.
[49] Yen TJ, Padilla WJ, Fang N, et al. Terahertz magnetic response from artificial materials. *Science*. 2004;303(5663):1494-1496.
[50] Linden S, Enkrich C, Wegener M, Zhou J, Koschny T, Soukoulis CM. Magnetic response of metamaterials at 100 terahertz. *Science*. 2004;306(5700):1351-1353.
[51] Soukoulis CM, Linden S, Wegener M. Negative refractive index at optical wavelengths. *Science*. 2007;315(5808):47-49.
[52] Zhang S, Fan W, Panoiu NC, Malloy KJ, Osgood RM, Brueck SRJ. Experimental demonstration of near-infrared negative-index metamaterials. *Phys Rev Lett*. 2005;95(13):137404.
[53] Dolling G, Enkrich C, Wegener M, Soukoulis CM, Linden S. Simultaneous negative phase and group velocity of light in a metamaterial. *Science*. 2006;312(5775):892-894.
[54] Zhang X, Liu Z. Superlenses to overcome the diffraction limit. *Nat Mater*. 2008;7(6):435-441.
[55] Pendry JB. Negative refraction makes a perfect lens. *Phys Rev Lett*. 2000;85(18):3966-3969.
[56] Grbic A, Eleftheriades GV. Overcoming the diffraction limit with a planar left-handed transmission-line lens. *Phys Rev Lett*. 2004;92(11):117403.
[57] Leonhardt U, Philbin TG. Transformation optics and the geometry of light. In: *Progress in Optics*. Vol 53. Elsevier; 2009:69-152.
[58] Chen H, Chan CT, Sheng P. Transformation optics and metamaterials. *Nat Mater*. 2010;9(5):387-396.
[59] Pendry JB, Aubry A, Smith DR, Maier SA. Transformation optics and subwavelength control of light. *Science*. 2012;337(6094):549-552.
[60] Leonhardt U. Optical conformal mapping. *Science*. 2006;312(5781):1777-1780.
[61] Li J, Pendry JB. Hiding under the carpet: a new strategy for cloaking. *Phys Rev Lett*. 2008;101(20):203901.
[62] Valentine J, Li J, Zentgraf T, Bartal G, Zhang X. An optical cloak made of dielectrics. *Nat Mater*. 2009;8(7):568-571.
[63] Gabrielli LH, Cardenas J, Poitras CB, Lipson M. Silicon nanostructure cloak operating at optical frequencies. *Nat Photonics*. 2009;3(8):461-463.
[64] Ergin T, Stenger N, Brenner P, Pendry JB, Wegener M. Three-dimensional invisibility cloak at optical wavelengths. *Science*. 2010;328(5976):337-339.
[65] Gharghi M, Gladden C, Zentgraf T, et al. A carpet cloak for visible light. *Nano Lett*. 2011;11(7):2825-2828.
[66] Zhang S, Genov DA, Sun C, Zhang X. Cloaking of matter waves. *Phys Rev Lett*. 2008;100(12):123002.
[67] Farhat M, Guenneau S, Enoch S. Ultrabroadband elastic cloaking in thin plates. *Phys Rev Lett*. 2009;103(2):24301.
[68] Zhang S, Xia C, Fang N. Broadband acoustic cloak for ultrasound waves. *Phys Rev Lett*. 2011;106(2):24301.
[69] Zigoneanu L, Popa BI, Cummer SA. Three-dimensional broadband omnidirectional acoustic ground cloak. *Nat Mater*. 2014;13(4):352-355.
[70] Xu H, Shi X, Gao F, Sun H, Zhang B. Ultrathin three-dimensional thermal cloak. *Phys Rev Lett*. 2014;112(5):54301.

[71] Park J, Youn JR, Song YS. Hydrodynamic metamaterial cloak for drag-free flow. *Phys Rev Lett*. 2019;123(7):74502.
[72] Lai Y, Ng J, Chen HY, Zhang ZQ, Chan CT. Illusion optics. *Front Phys China*. 2010;5(3):308-318.
[73] Sheng C, Bekenstein R, Liu H, Zhu S, Segev M. Wavefront shaping through emulated curved space in waveguide settings. *Nat Commun*. 2016;7(1):1-8.
[74] Ni X, Ishii S, Kildishev AV, Shalaev VM. Ultra-thin, planar, Babinet-inverted plasmonic metalenses. *Light Sci Appl*. 2013;2(4):e72.
[75] Decker M, Staude I, Falkner M, et al. High-efficiency dielectric Huygens' surfaces. *Adv Opt Mater*. 2015;3(6):813-820.
[76] Huang L, Chen X, Mühlenbernd H, et al. Dispersionless phase discontinuities for controlling light propagation. *Nano Lett*. 2012;12(11):5750-5755.
[77] Arbabi A, Horie Y, Ball AJ, Bagheri M, Faraon A. Subwavelength-thick lenses with high numerical apertures and large efficiency based on high-contrast transmitarrays. *Nat Commun*. 2015;6(1):1-6.
[78] Wang S, Wu PC, Su VC, et al. Broadband achromatic optical metasurface devices. *Nat Commun*. 2017;8:1-9.
[79] Mueller JPB, Rubin NA, Devlin RC, Groever B, Capasso F. Metasurface polarization optics: independent phase control of arbitrary orthogonal states of polarization. *Phys Rev Lett*. 2017;118(11):113901.
[80] Sun S, He Q, Xiao S, Xu Q, Li X, Zhou L. Gradient-index meta-surfaces as a bridge linking propagating waves and surface waves. *Nat Mater*. 2012;11(5):426-431.
[81] Chen J, Li T, Wang S, Zhu S. Multiplexed holograms by surface plasmon propagation and polarized scattering. *Nano Lett*. 2017;17(8):5051-5055.
[82] Chen J, Chen X, Li T, Zhu S. On-chip detection of orbital angular momentum beam by plasmonic nanogratings. *Laser Photon Rev*. 2018;12(8):1700331.
[83] Shamkhi HK, Baryshnikova KV, Sayanskiy A, et al. Transverse scattering and generalized Kerker effects in all-dielectric Mie-resonant metaoptics. *Phys Rev Lett*. 2019;122(19):193905.
[84] Shitrit N, Bretner I, Gorodetski Y, Kleiner V, Hasman E. Optical spin Hall effects in plasmonic chains. *Nano Lett*. 2011;11(5):2038-2042.
[85] Kang M, Chen J, Wang XL, Wang HT. Twisted vector field from an inhomogeneous and anisotropic metamaterial. *J Opt Soc Am B*. 2012;29(4):572-576.
[86] Kang M, Feng T, Wang HT, Li J. Wave front engineering from an array of thin aperture antennas. *Opt Express*. 2012;20(14):15882-15890.
[87] Huang L, Chen X, Mühlenbernd H, et al. Three-dimensional optical holography using a plasmonic metasurface. *Nat Commun*. 2013;4(1):1-8.
[88] Zheng G, Mühlenbernd H, Kenney M, Li G, Zentgraf T, Zhang S. Metasurface holograms reaching 80% efficiency. *Nat Nanotechnol*. 2015;10(4):308-312.
[89] Li J, Yuan Y, Wu Q, Burokur SN, Zhang K. Dual-band independent phase control based on high efficiency metasurface. *Chin Opt Lett*. 2021;19(10):100501.
[90] Chen C, Song W, Chen JW, et al. Spectral tomographic imaging with aplanatic metalens. *Light Sci Appl*. 2019;8(1):1-8.
[91] Fang B, Wang Z, Gao S, Zhu S, Li T. Manipulating guided wave radiation with integrated geometric metasurface. *Nanophotonics*. 2022;11(9):1923-1930.
[92] Hsiao H, Chu CH, Tsai DP. Fundamentals and applications of metasurfaces. *Small Methods*. 2017;1(4):1600064.
[93] Kamali SM, Arbabi E, Arbabi A, Faraon A. A review of dielectric optical metasurfaces for wavefront control. *Nanophotonics*. 2018;7(6):1041-1068.
[94] Faraji-Dana M, Arbabi E, Arbabi A, Kamali SM, Kwon H, Faraon A. Compact folded metasurface spectrometer. *Nat Commun*. 2018;9(1):1-8.
[95] Arbabi E, Kamali SM, Arbabi A, Faraon A. Vectorial holograms with a dielectric metasurface: ultimate polarization pattern generation. *ACS Photonics*. 2019;6(11):2712-2718.
[96] Faraji-Dana M, Arbabi E, Kwon H, et al. Hyperspectral imager with folded metasurface optics. *ACS Photonics*. 2019;6(8):2161-2167.
[97] Kamali SM, Arbabi E, Faraon A. Metasurface-based compact light engine for AR headsets. In: *Optical Design Challenge*. Vol 11040. SPIE; 2019:1104002.
[98] Kamali SM, Arbabi E, Kwon H, Faraon A. Metasurface-generated complex 3-dimensional optical fields for interference lithography. *Proc Natl Acad Sci*. 2019;116(43):21379-21384.
[99] Fan ZB, Shao ZK, Xie MY, et al. Silicon nitride metalenses for close-to-one numerical aperture and wide-angle visible imaging. *Phys Rev Appl*. 2018;10(1):14005.
[100] Arbabi A, Horie Y, Bagheri M, Faraon A. Dielectric metasurfaces for complete control of phase and polarization with subwavelength spatial resolution and high transmission. *Nat Nanotechnol*. 2015;10(11):937-943.
[101] Wang H, Zhang Z, Zhao K, Liu W, Wang P, Lu Y. Independent phase manipulation of co- and cross-polarizations with all-dielectric metasurface. *Chin Opt Lett*. 2021;19(5):53601.
[102] Fan Q, Liu M, Zhang C, et al. Independent amplitude control of arbitrary orthogonal states of polarization via dielectric metasurfaces. *Phys Rev Lett*. 2020;125(26):267402.
[103] Li T. New opportunities for metalenses in imaging applications. *Sci China: Phys Mech Astron*. 2020;63:284231.
[104] Chen X, Huang L, Mühlenbernd H, et al. Dual-polarity plasmonic metalens for visible light. *Nat Commun*. 2012;3(1):1-6.
[105] Monticone F, Estakhri NM, Alu A. Full control of nanoscale optical transmission with a composite metascreen. *Phys Rev Lett*. 2013;110(20):203903.
[106] Arbabi A, Faraon A. Fundamental limits of ultrathin metasurfaces. *Sci Rep*. 2017;7(1):1-9.
[107] Khorasaninejad M, Chen WT, Devlin RC, Oh J, Zhu AY, Capasso F. Metalenses at visible wavelengths: diffraction-limited focusing and subwavelength resolution imaging. *Science*. 2016;352(6290):1190-1194.
[108] Avayu O, Almeida E, Prior Y, Ellenbogen T. Composite functional metasurfaces for multispectral achromatic optics. *Nat Commun*. 2017;8(1):1-7.
[109] Lin D, Holsteen AL, Maguid E, et al. Photonic multitasking interleaved Si nanoantenna phased array. *Nano Lett*. 2016;16(12):7671-7676.

[110] Li L, Yuan Q, Chen R, et al. Chromatic dispersion manipulation based on metasurface devices in the mid-infrared region. *Chin Opt Lett*. 2020;18(8):82401.
[111] Arbabi E, Arbabi A, Kamali SM, Horie Y, Faraon A. Multiwavelength polarization-insensitive lenses based on dielectric metasurfaces with meta-molecules. *Optica*. 2016;3(6):628-633.
[112] Khorasaninejad M, Aieta F, Kanhaiya P, et al. Achromatic metasurface lens at telecommunication wavelengths. *Nano Lett*. 2015;15(8):5358-5362.
[113] Aieta F, Kats MA, Genevet P, Capasso F. Multiwavelength achromatic metasurfaces by dispersive phase compensation. *Science*. 2015;347(6228):1342-1345.
[114] Arbabi E, Arbabi A, Kamali SM, Horie Y, Faraon A. High efficiency double-wavelength dielectric metasurface lenses with dichroic birefringent meta-atoms. *Opt Express*. 2016;24(16):18468-18477.
[115] Khorasaninejad M, Shi Z, Zhu AY, et al. Achromatic metalens over 60 nm bandwidth in the visible and metalens with reverse chromatic dispersion. *Nano Lett*. 2017;17(3):1819-1824.
[116] Arbabi E, Arbabi A, Kamali SM, Horie Y, Faraon A. Controlling the sign of chromatic dispersion in diffractive optics with dielectric metasurfaces. *Optica*. 2017;4(6):625-632.
[117] Chen WT, Zhu AY, Sanjeev V, et al. A broadband achromatic metalens for focusing and imaging in the visible. *Nat Nanotechnol*. 2018;13(3):220-226.
[118] Arbabi A, Arbabi E, Kamali SM, Horie Y, Han S, Faraon A. Miniature optical planar camera based on a wide-angle metasurface doublet corrected for monochromatic aberrations. *Nat Commun*. 2016;7(1):1-9.
[119] Martins A, Li K, Li J, et al. On metalenses with arbitrarily wide field of view. *ACS Photonics*. 2020;7(8):2073-2079.
[120] Zhang F, Pu M, Li X, et al. Extreme-angle silicon infrared optics enabled by streamlined surfaces. *Adv Mater*. 2021;33(11):2008157.
[121] Chen J, Ye X, Gao S, et al. Planar wide-angle-imaging camera enabled by metalens array. *Optica*. 2022;9(4):431-437.
[122] Wang S, Wu PC, Su VC, et al. A broadband achromatic metalens in the visible. *Nat Nanotechnol*. 2018;13(3):227-232.
[123] Lin RJ, Su VC, Wang S, et al. Achromatic metalens array for full-colour light-field imaging. *Nat Nanotechnol*. 2019;14(3):227-231.
[124] Luo X, Zhang F, Pu M, Guo Y, Li X, Ma X. Recent advances of wide-angle metalenses: principle, design, and applications. *Nanophotonics*. 2022;11(1):1-20.
[125] Lin Z, Groever B, Capasso F, Rodriguez AW, Lončar M. Topology-optimized multilayered metaoptics. *Phys Rev Appl*. 2018;9(4):44030.
[126] Hao C, Gao S, Ruan Q, et al. Single-layer aberration-compensated flat lens for robust wide-angle imaging. *Laser Photon Rev*. 2020;14(6):2000017.
[127] Pu M, Li X, Guo Y, Ma X, Luo X. Nanoapertures with ordered rotations: symmetry transformation and wide-angle flat lensing. *Opt Express*. 2017;25(25):31471-31477.
[128] Lassalle E, Mass TWW, Eschimese D, et al. Imaging properties of large field-of-view quadratic metalenses and their applications to fingerprint detection. *ACS Photonics*. 2021;8(5):1457-1468.
[129] Shalaginov MY, An S, Yang F, et al. Single-element diffraction-limited fisheye metalens. *Nano Lett*. 2020;20(10):7429-7437.
[130] Fan CY, Lin CP, Su GDJ. Ultrawide-angle and high-efficiency metalens in hexagonal arrangement. *Sci Rep*. 2020;10(1):1-9.
[131] Engelberg J, Zhou C, Mazurski N, Bar-David J, Kristensen A, Levy U. Near-IR wide-field-of-view Huygens metalens for outdoor imaging applications. *Nanophotonics*. 2020;9(2):361-370.
[132] Groever B, Chen WT, Capasso F. Meta-lens doublet in the visible region. *Nano Lett*. 2017;17(8):4902-4907.
[133] Achouri K, Caloz C. Design, concepts, and applications of electromagnetic metasurfaces. *Nanophotonics*. 2018;7(6):1095-1116.
[134] Shen B, Wang P, Polson R, Menon R. An integrated-nanophotonics polarization beamsplitter with $2.4 \times 2.4\ \mu m^2$ footprint. *Nat Photonics*. 2015;9(6):378-382.
[135] Sell D, Yang J, Doshay S, Yang R, Fan JA. Large-angle, multifunctional metagratings based on freeform multimode geometries. *Nano Lett*. 2017;17(6):3752-3757.
[136] Bendsoe MP, Sigmund O. *Topology Optimization: Theory, Methods, and Applications*. Springer Science & Business Media; 2003.
[137] Jensen JS, Sigmund O. Topology optimization for nano-photonics. *Laser Photon Rev*. 2011;5(2):308-321.
[138] Li J, Cao M, Liang W, Zhang Y, Xie Z, Yuan X. Inverse design of 1D color splitter for high-efficiency color imaging. *Chin Opt Lett*. 2022;20(7):73601.
[139] Su L, Piggott AY, Sapra NV, Petykiewicz J, Vuckovic J. Inverse design and demonstration of a compact on-chip narrowband three-channel wavelength demultiplexer. *ACS Photonics*. 2018;5(2):301-305.
[140] Holland JH. Genetic algorithms. *Sci Am*. 1992;267(1):66-73.
[141] Dorigo M, Birattari M, Stutzle T. Ant colony optimization. *IEEE Comput Intell Mag*. 2006;1(4):28-39.
[142] Lin Z, Liu V, Pestourie R, Johnson SG. Topology optimization of freeform large-area metasurfaces. *Opt Express*. 2019;27(11):15765-15775.
[143] Phan T, Sell D, Wang EW, et al. High-efficiency, large-area, topology-optimized metasurfaces. *Light Sci Appl*. 2019;8(1):1-9.
[144] Wang EW, Sell D, Phan T, Fan JA. Robust design of topology-optimized metasurfaces. *Opt Mater Express*. 2019;9(2):469-482.
[145] Fliege J, Drummond LMG, Svaiter BF. Newton's method for multiobjective optimization. *SIAM J Optim*. 2009;20(2):602-626.
[146] Désidéri JA. Multiple-gradient descent algorithm (MGDA) for multiobjective optimization. *Comptes Rendus Math*. 2012;350(5-6):313-318.
[147] Jordan MI, Mitchell TM. Machine learning: trends, perspectives, and prospects. *Science*. 2015;349(6245):255-260.
[148] Sra S, Nowozin S, Wright SJ. *Optimization for Machine Learning*. MIT Press; 2012.
[149] Alzubi J, Nayyar A, Kumar A. Machine learning from theory to algorithms: an overview. *J Phys Conf Ser*. 2018;1142:012012.
[150] Carleo G, Cirac I, Cranmer K, et al. Machine learning and the physical sciences. *Rev Mod Phys*. 2019;91(4):45002.
[151] Mahesh B. Machine learning algorithms—a review. *Int J Sci Res (IJSR)[Internet]*. 2020;9:381-386.

[152] Deng L, Hinton G, Kingsbury B. New types of deep neural network learning for speech recognition and related applications: an overview. In: *2013 IEEE International Conference on Acoustics, Speech and Signal Processing*. IEEE; 2013:8599-8603.
[153] Eitel A, Springenberg JT, Spinello L, Riedmiller M, Burgard W. Multimodal deep learning for robust RGB-D object recognition. In: *2015 IEEE/RSJ International Conference on Intelligent Robots and Systems (IROS)*. IEEE; 2015: 681-687.
[154] Voulodimos A, Doulamis N, Doulamis A, Protopapadakis E. Deep learning for computer vision: a brief review. *Comput Intell Neurosci*. 2018;2018:7068349.
[155] Zhao ZQ, Zheng P, Xu St, Wu X. Object detection with deep learning: a review. *IEEE Trans Neural Networks Learn Syst*. 2019;30(11):3212-3232.
[156] Grigorescu S, Trasnea B, Cocias T, Macesanu G. A survey of deep learning techniques for autonomous driving. *J Field Rob*. 2020;37(3):362-386.
[157] LeCun Y, Bengio Y, Hinton G. Deep learning. *Nature*. 2015;521(7553):436-444.
[158] Goodfellow I, Bengio Y, Courville A. *Deep Learning*. MIT Press; 2016.
[159] Hemmatyar O, Abdollahramezani S, Kiarashinejad Y, Zandehshahvar M, Adibi A. Full color generation with fano-type resonant HfO_2 nanopillars designed by a deep-learning approach. *Nanoscale*. 2019;11(44):21266-21274.
[160] So S, Mun J, Rho J. Simultaneous inverse design of materials and structures via deep learning: demonstration of dipole resonance engineering using core–shell nanoparticles. *ACS Appl Mater Interfaces*. 2019;11(27):24264-24268.
[161] Rivenson Y, Zhang Y, Günaydın H, Teng D, Ozcan A. Phase recovery and holographic image reconstruction using deep learning in neural networks. *Light Sci Appl*. 2018;7(2):17141.
[162] Wiecha PR, Lecestre A, Mallet N, Larrieu G. Pushing the limits of optical information storage using deep learning. *Nat Nanotechnol*. 2019;14(3):237-244.
[163] Li L, Shuang Y, Ma Q, et al. Intelligent metasurface imager and recognizer. *Light Sci Appl*. 2019;8(1):1-9.
[164] Qian C, Zheng B, Shen Y, et al. Deep-learning-enabled self-adaptive microwave cloak without human intervention. *Nat Photonics*. 2020;14(6):383-390.
[165] Peurifoy J, Shen Y, Jing L, et al. Nanophotonic particle simulation and inverse design using artificial neural networks. *Sci Adv*. 2018;4(6):eaar4206.
[166] Hu B, Wu B, Tan D, Xu J, Chen Y. Robust inverse-design of scattering spectrum in core–shell structure using modified denoising autoencoder neural network. *Opt Express*. 2019;27(25):36276-36285.
[167] Wiecha PR, Muskens OL. Deep learning meets nanophotonics: a generalized accurate predictor for near fields and far fields of arbitrary 3D nanostructures. *Nano Lett*. 2019;20(1):329-338.
[168] Vahidzadeh E, Shankar K. Artificial neural Network-based prediction of the optical properties of spherical core–shell plasmonic metastructures. *Nanomaterials*. 2021;11(3):633.
[169] An X, Cao Y, Wei Y, et al. Broadband achromatic metalens design based on deep neural networks. *Opt Lett*. 2021; 46(16):3881-3884.
[170] Fan CY, Su GDJ. Time-effective simulation methodology for broadband achromatic metalens using deep neural networks. *Nanomaterials*. 2021;11(8):1966.
[171] Gu Y, Hao R, Li EP. Independent bifocal metalens design based on deep learning algebra. *IEEE Photonics Technol Lett*. 2021;33(8):403-406.
[172] Zarei S, Khavasi A. Inverse design of on-chip thermally tunable varifocal metalens based on silicon metalines. *IEEE Access*. 2021;9:73453-73466.
[173] Wu Y, Luo Y, Chaudhari G, et al. Bright-field holography: cross-modality deep learning enables snapshot 3D imaging with bright-field contrast using a single hologram. *Light Sci Appl*. 2019;8(1):1-7.
[174] Ren H, Shao W, Li Y, Salim F, Gu M. Three-dimensional vectorial holography based on machine learning inverse design. *Sci Adv*. 2020;6(16):eaaz4261.
[175] Liu C, Yu WM, Ma Q, Li L, Cui TJ. Intelligent coding metasurface holograms by physics-assisted unsupervised generative adversarial network. *Photonics Res*. 2021;9(4):B159-B167.
[176] Ma W, Xu Y, Xiong B, et al. Pushing the limits of functionality-multiplexing capability in metasurface design based on statistical machine learning. *Adv Mater*. 2022;34:e2110022.
[177] Ma D, Li Z, Liu W, et al. Deep-learning enabled multicolor meta-holography. *Adv Opt Mater*. 2022;10:2102628.
[178] Sajedian I, Lee H, Rho J. Double-deep Q-learning to increase the efficiency of metasurface holograms. *Sci Rep*. 2019;9(1):1-8.
[179] Keshavarz Hedayati M, Elbahri M. Review of metasurface plasmonic structural color. *Plasmonics*. 2017;12(5):1463-1479.
[180] Yang B, Cheng H, Chen S, Tian J. Structural colors in metasurfaces: principle, design and applications. *Mater Chem Front*. 2019;3(5):750-761.
[181] Gao L, Li X, Liu D, Wang L, Yu Z. A bidirectional deep neural network for accurate silicon color design. *Adv Mater*. 2019;31(51):1905467.
[182] Sajedian I, Badloe T, Rho J. Optimisation of colour generation from dielectric nanostructures using reinforcement learning. *Opt Express*. 2019;27(4):5874-5883.
[183] González-Alcalde AK, Salas-Montiel R, Kalt V, Blaize S, Macías D. Engineering colors in all-dielectric metasurfaces: metamodeling approach. *Opt Lett*. 2020;45(1):89-92.
[184] Kalt V, González-Alcalde AK, Es-Saidi S, Salas-Montiel R, Blaize S, Macías D. Metamodeling of high-contrast-index gratings for color reproduction. *J Opt Soc Am A*. 2019;36(1): 79-88.
[185] Lee T, Jang J, Jeong H, Rho J. Plasmonic- and dielectric-based structural coloring: from fundamentals to practical applications. *Nano Convergence*. 2018;5(1):1-21.
[186] Baxter J, Calà Lesina A, Guay JM, Weck A, Berini P, Ramunno L. Plasmonic colours predicted by deep learning. *Sci Rep*. 2019;9(1):1-9.
[187] Roberts NB, Keshavarz Hedayati M. A deep learning approach to the forward prediction and inverse design of plasmonic metasurface structural color. *Appl Phys Lett*. 2021;119(6):61101.
[188] Siegel J, Wang AY, Menabde SG, Kats MA, Jang MS, Brar VW. Self-stabilizing laser sails based on optical metasurfaces. *ACS Photonics*. 2019;6(8):2032-2040.

[189] Salary MM, Mosallaei H. Photonic metasurfaces as relativistic light sails for Doppler-broadened stable beam-riding and radiative cooling. *Laser Photon Rev*. 2020;14(8):1900311.
[190] Han C, Zhang B, Wang H, Ding J. Metamaterial perfect absorber with morphology-engineered meta-atoms using deep learning. *Opt Express*. 2021;29(13):19955-19963.
[191] Tittl A, John-Herpin A, Leitis A, Arvelo ER, Altug H. Metasurface-based molecular biosensing aided by artificial intelligence. *Angew Chemie Int Ed*. 2019;58(42): 14810-14822.
[192] Moon G, Choi J-r, Lee C, Oh Y, Kim KH, Kim D. Machine learning-based design of meta-plasmonic biosensors with negative index metamaterials. *Biosens Bioelectron*. 2020;164: 112335.
[193] Wang Y, Li M, Wang Y. Silk: a versatile biomaterial for advanced optics and photonics. *Chin Opt Lett*. 2020;18(8): 80004.
[194] John-Herpin A, Kavungal D, von Mücke L, Altug H. Infrared metasurface augmented by deep learning for monitoring dynamics between all major classes of biomolecules. *Adv Mater*. 2021;33(14):2006054.
[195] Kudyshev ZA, Kildishev AV, Shalaev VM, Boltasseva A. Machine-learning-assisted metasurface design for high-efficiency thermal emitter optimization. *Appl Phys Rev*. 2020;7(2):21407.
[196] Cui TJ, Qi MQ, Wan X, Zhao J, Cheng Q. Coding metamaterials, digital metamaterials and programmable metamaterials. *Light Sci Appl*. 2014;3(10):e218.
[197] Li L, Cui TJ. Information metamaterials—from effective media to real-time information processing systems. *Nanophotonics*. 2019;8(5):703-724.
[198] Li L, Jun Cui T, Ji W, et al. Electromagnetic reprogrammable coding-metasurface holograms. *Nat Commun*. 2017;8(1):1-7.
[199] Li L, Ruan H, Liu C, et al. Machine-learning reprogrammable metasurface imager. *Nat Commun*. 2019;10(1):1-8.
[200] Zhao J. A survey of intelligent reflecting surfaces (IRSs): towards 6G wireless communication networks. *arXiv Prepr arXiv190704789*. 2019.
[201] Huang C, Zappone A, Alexandropoulos GC, Debbah M, Yuen C. Reconfigurable intelligent surfaces for energy efficiency in wireless communication. *IEEE Trans Wireless Commun*. 2019;18(8):4157-4170.
[202] Liaskos C, Tsioliaridou A, Nie S, Pitsillides A, Ioannidis S, Akyildiz I. An interpretable neural network for configuring programmable wireless environments. In: *2019 IEEE 20th International Workshop on Signal Processing Advances in Wireless Communications (SPAWC)*. IEEE; 2019:1-5.
[203] Taha A, Alrabeiah M, Alkhateeb A. Enabling large intelligent surfaces with compressive sensing and deep learning. *IEEE Access*. 2021;9:44304-44321.
[204] Zhang X, Li Q, Liu F, et al. Controlling angular dispersions in optical metasurfaces. *Light Sci Appl*. 2020;9(1):1-12.
[205] Verre R, Svedendahl M, Odebo Länk N, et al. Directional light extinction and emission in a metasurface of tilted plasmonic nanopillars. *Nano Lett*. 2016;16(1):98-104.
[206] Presutti F, Monticone F. Focusing on bandwidth: achromatic metalens limits. *Optica*. 2020;7(6):624-631.
[207] Banerji S, Meem M, Majumder A, Vasquez FG, Sensale-Rodriguez B, Menon R. Imaging with flat optics: metalenses or diffractive lenses? *Optica*. 2019;6(6):805-810.
[208] Saha S, Shah D, Shalaev VM, Boltasseva A. Tunable metasurfaces: controlling light in space and time. *Opt Photonics News*. 2021;32(7):34-41.
[209] Arbabi E, Arbabi A, Kamali SM, Horie Y, Faraji-Dana M, Faraon A. MEMS-tunable dielectric metasurface lens. *Nat Commun*. 2018;9(1):1-9.
[210] Li J, Yu P, Zhang S, Liu N. Electrically-controlled digital metasurface device for light projection displays. *Nat Commun*. 2020;11(1):1-7.
[211] Ding F, Yang Y, Bozhevolnyi SI. Dynamic metasurfaces using phase-change chalcogenides. *Adv Opt Mater*. 2019; 7(14):1801709.
[212] Zhang Y, Fowler C, Liang J, et al. Electrically reconfigurable non-volatile metasurface using low-loss optical phase-change material. *Nat Nanotechnol*. 2021;16(6):661-666.
[213] Shalaginov MY, An S, Zhang Y, et al. Reconfigurable all-dielectric metalens with diffraction-limited performance. *Nat Commun*. 2021;12(1):1-8.
[214] Park J, Jeong BG, Kim SI, et al. All-solid-state spatial light modulator with independent phase and amplitude control for three-dimensional LiDAR applications. *Nat Nanotechnol*. 2021;16(1):69-76.
[215] Qian C, Chen H. A perspective on the next generation of invisibility cloaks—intelligent cloaks. *Appl Phys Lett*. 2021;118(18):180501.
[216] Liu Z, Zhu D, Rodrigues SP, Lee KT, Cai W. Generative model for the inverse design of metasurfaces. *Nano Lett*. 2018;18(10):6570-6576.
[217] Melati D, Grinberg Y, Kamandar Dezfouli M, et al. Mapping the global design space of nanophotonic components using machine learning pattern recognition. *Nat Commun*. 2019;10(1):1-9.
[218] Jiang J, Fan JA. Global optimization of dielectric metasurfaces using a physics-driven neural network. *Nano Lett*. 2019;19(8):5366-5372.
[219] Barbastathis G, Ozcan A, Situ G. On the use of deep learning for computational imaging. *Optica*. 2019;6(8):921-943.
[220] Zuo C, Qian J, Feng S, et al. Deep learning in optical metrology: a review. *Light Sci Appl*. 2022;11(1):1-54.
[221] Zhang Q, Yu H, Barbiero M, Wang B, Gu M. Artificial neural networks enabled by nanophotonics. *Light Sci Appl*. 2019;8(1):1-14.
[222] Lin X, Rivenson Y, Yardimci NT, et al. All-optical machine learning using diffractive deep neural networks. *Science*. 2018;361(6406):1004-1008.
[223] Goi E, Chen X, Zhang Q, et al. Nanoprinted high-neuron-density optical linear perceptrons performing near-infrared inference on a CMOS chip. *Light Sci Appl*. 2021;10(1):1-11.
[224] Qian C, Lin X, Lin X, et al. Performing optical logic operations by a diffractive neural network. *Light Sci Appl*. 2020;9(1):1-7.
[225] Liu C, Ma Q, Luo ZJ, et al. A programmable diffractive deep neural network based on a digital-coding metasurface array. *Nat Electron*. 2022;5(2):113-122.
[226] Zhou T, Lin X, Wu J, et al. Large-scale neuromorphic optoelectronic computing with a reconfigurable diffractive processing unit. *Nat Photonics*. 2021;15(5):367-373.

[227] Shen Y, Harris NC, Skirlo S, et al. Deep learning with coherent nanophotonic circuits. *Nat Photonics*. 2017;11(7):441-446.
[228] Shastri BJ, Tait AN, Ferreira de Lima T, et al. Photonics for artificial intelligence and neuromorphic computing. *Nat Photonics*. 2021;15(2):102-114.
[229] Luo X, Hu Y, Li X, et al. Metasurface-enabled on-chip multiplexed diffractive neural networks in the visible. *arXiv Prepr arXiv210707873*. 2021.
[230] Zuo Y, Li B, Zhao Y, et al. All-optical neural network with nonlinear activation functions. *Optica*. 2019;6(9):1132-1137.
[231] Mengu D, Luo Y, Rivenson Y, Lin X, Veli M, Ozcan A. Response to Comment on "All-optical machine learning using diffractive deep neural networks". *arXiv Prepr arXiv181004384*. 2018.
[232] Spreyer F, Zhao R, Huang L, Zentgraf T. Second harmonic imaging of plasmonic Pancharatnam–Berry phase metasurfaces coupled to monolayers of WS_2. *Nanophotonics*. 2020;9(2):351-360.
[233] Staude I, Pertsch T, Kivshar YS. All-dielectric resonant meta-optics lightens up. *ACS Photonics*. 2019;6(4):802-814.
[234] Hu G, Hong X, Wang K, et al. Coherent steering of nonlinear chiral valley photons with a synthetic Au–WS_2 metasurface. *Nat Photonics*. 2019;13(7):467-472.
[235] Li L, Liu Z, Ren X, et al. Metalens-array-based high-dimensional and multiphoton quantum source. *Science*. 2020;368(6498):1487-1490.
[236] Xie YY, Ni PN, Wang QH, et al. Metasurface-integrated vertical cavity surface-emitting lasers for programmable directional lasing emissions. *Nat Nanotechnol*. 2020;15(2):125-130.

AUTHOR BIOGRAPHIES

Ji Chen is an Associate Research Fellow and Master Supervisor at Southeast University. He received his B.S. degree in Material Physics in 2014 and Ph.D. degree in Optical Engineering in 2019, both from Nanjing University. From 2019 to 2021, he has two working experiences in China Electronics Technology Group Corporation and College of Engineering and Applied Science, Nanjing University. He is now working in School of Information Science and Engineering, National Mobile Communications Research Laboratory, Southeast University. His research results have been published in Nature, Nature Nanotechnology, Nature Communications, Optica, Laser & Photonics Reviews, and so forth. His research interests include metaoptics, optical wireless communications, advanced imaging technology, and surface plasmon photonics.

Shanshan Hu is a Postgraduate at Nanjing University. She received her B.E. degree in Optoelectronic Information Science and Engineering at China University of Petroleum. She joined the National Laboratory of Solid State Microstructures at Nanjing University to pursue her M.S. degree under the guidance of Prof. Shining Zhu and Prof. Tao Li. Her current research interests focus on the metadevices design and metalens imaging technology.

Shining Zhu is a Professor at School of Physics and Principal Investigator (PI) at the National Laboratory of Solid State Microstructures, Nanjing University. He is also an Academician of the CAS, and a Fellow of OSA, COS, and APS. He got his Master's and Ph.D. degrees from the Physics Department of Nanjing University. His main research interests are functionally microstructured materials, including their applications on laser, nonlinear optics, quantum optics, quantum information, and so forth.

Tao Li is a Professor at Nanjing University. He received his Ph.D. degree at NJU in 2005 and joined NJU as a faculty in 2008. He worked as a visiting scholar at Nanyang Technology University, Singapore, in 2012, and Hong Kong Baptist University under the support of "K.C. Wong Education Foundation" scholarship in 2013. He was selected as the "Dengfeng Talent Program B" from Nanjing University, won the "National Funds for Outstanding Young Scientists" and "Young and middle-aged leading scientists" from MOST. His research interest is about the metamaterials, plasmonics, and photonic integration. Till now, he has published >100 papers with citations of over 5000 and a recent H index of 36 (Web of Science), and presented >50 invited talks at international conferences and seminars.

How to cite this article: Chen J, Hu S, Zhu S, Li T. Metamaterials: from fundamental physics to intelligent design. *Interdiscip Mater*. 2022;1-25. doi:10.1002/idm2.12049